Addis Ababa University

Addis Ababa Institution of Technology

School of Mechanical and Industrial Engineering

Free Vibration Study on Edge Cracked Glass Fiber Reinforced Polymer Laminate

By Mulatu Achenef

Addis Ababa, Ethiopia

2019

Addis Ababa University

Addis Ababa Institute of Technology

School of Mechanical and Industrial Engineering

Free Vibration Study on Edge Cracked Glass Fiber Reinforced Polymer Laminate

By:

Mulatu Achenef

Adviser: Ermias G. Koricho (Ph.D.)

Co-Adviser: Araya Abera (PhD. Candidate)

A Thesis submitted at Addis Ababa Institute of Technology in partial fulfillment of the requirements for the Degree of Master of Science in Mechanical Engineering.

Specialization in mechanical design

Addis Ababa

2019

The undersigned have examined the thesis entitled '***Free Vibration Study on edge Cracked Glass Fiber Reinforced Polymer laminate***' presented by Mulatu Achenef. A candidate for the degree of Master of Science and hereby certifies that it is worthy of acceptance.

Approved by Board of examiners:

_____	_____	_____
Chair man of the school	Signature	Date
Ermias G. Koricho (Ph.D.)	_____	_____
Advisor	Signature	Date
Araya Abera (PhD. Candidate)	_____	_____
Co-Advisor	Signature	Date
_____	_____	_____
Internal Examiner	Signature	Date
_____	_____	_____
External Examiner	Signature	Date

Declaration

I certify that the research work titled "***Free Vibration Study on edge Cracked Glass Fiber Reinforced Polymer laminate***" is my own original work and it has not been presented elsewhere for assessment.

Mulatu Achenef	_____	_____
Student	Signature	Date
Ermias G. Koricho (Ph.D.)	_____	_____
Advisor	Signature	Date
Araya Abera (PhD. Candidate)	_____	_____
Co-Advisor	Signature	Date

Acknowledgments

First, I would like to express my deepest gratitude to the almighty Jesus Christ and his mother St Mary for all the things they gave me and make all the things possible.

Second, my special thanks go to my advisor Ermias Gebrekidan (Ph.D.), Assistant professor mechanical engineering Georgia Southern University, for his continuous support in advising, teaching and giving his time for assessment of my research work.

Third, my appreciation is to the Dejen Aviation industry, unmanned air vehicle department staff, especially for doll and Melaku for their support by providing all the necessary material and equipment for the manufacturing of composite material by vacuum bagging method.

I would also like to thank Mr. Araya, design stream chair of Addis Ababa University, for his support on my research work and all staff members of the school of mechanical and industrial engineering for their encouragement and support

Finally, I have to express my gratitude to my father, mother, sisters, and brothers for their limitless support and continuous encouragement throughout my life and my friends for their support to finish my research work.

Abstract

The fiberglass-reinforced polymer is the most widely used composite because of its low cost and easy availability in the market. Fiberglass reinforced polymer is used for structural and semi-structural body parts of the automotive. During services, crack is the most common defect in a structure and cracked composite laminate is subjected to dynamic load and the vibration of the cracked laminate has a significant effect on the failure of the structure. A crack on a laminate reduces the stiffness of the structure and the change of stiffness affects the vibration properties of the laminate. During a change in vibration properties of the laminate resonance will occur and that causes catastrophic failure. In this study, the free vibration analysis, particularly the natural frequency of edge cracked glass fiber reinforced polymer laminate using Analytical, Numerical by using Abaqus software and Experimental analysis was studied. Specimen were prepared using a vacuum bagging assisted hand layup method. ASTM E756 is used for free vibration analysis. Experiments are conducted using unidirectional [04]s and quasi-isotropic [0,90,45, -45]s laminated beam with different crack introduced by a hacksaw. The effect of crack depth and crack location on natural frequencies of unidirectional [04]s and quasi-isotropic [0,90,45, -45]laminated beam investigated for a cantilever beam. Results showed that the natural frequencies were different for unidirectional laminate and quasi-isotropic laminate and it indicates the vibration properties of composite material depend on fiber arrangement. For both UD and QS laminate crack decrease the natural frequency. From the analysis the natural frequency decrease for an increase of crack depth. For both UD and QS laminates the location of the crack affected the natural frequency. The effect of crack depth and crack location on the change of the natural frequency showed the same trend in all the three methods.

Keywords: Unidirectional laminate, Quasi-Isotropic laminate, edge crack, natural frequency

Contents

Lists of figures

List of tables

Nomenclature

ρ_f = Density of Fiber (g/cc)

ρ_m = Density of Matrix (g/cc)

W_f = weight of Fiber (g)

W_m = weight of Matrix (g)

Wc = weight of composite specimen (g)

V_f = Volume of fibers, (cm^3)

V_m = Volume of matrix, (cm^3)

V_C = Volume of Composite mold (cm^3)

v_F = Fibers Volume fraction

v_m = Matrix Volume fraction

W_F = Fiber weight fraction

W_M = Matrix weight fraction

E1= longitudinal modulus of elasticity

E2= transverse modulus of elasticity

G12= Shear modulus (MPa)

List of Abbreviations and Acronyms

GFRP	Glass fiber reinforced polymer
QI	Quasi-Isotropic
UI	Unidirectional
ANA	Analytical method
NUM	Numerical method
EXP	Experimental method
FRF	frequency response function
ASTM	America Society for Testing and Material
NF	Natural frequency
L	length of the beam
Lc	crack location
a	crack depth
b	width
h	height
Eq.	Equation
cc	Cubic centimeter
VBAHT	Vacuum bagging Assisted Hand Lay-up technique
mm	millimeter

Chapter One

Introduction

1.1. Background

Any motion that repeats itself after some interval of time is called vibration. Vibrations are oscillations of a mechanical or structural system about an equilibrium position. Many machine elements are subjected to a different vibration. The vibration on the mechanical element will be necessary for doing some work or distractive type. In engineering design, the main concern is decreasing vibration and the frequency of the vibration should never be equal to the natural frequency because it causes catastrophic failure. (Rao, no date) As technology grows engineering structures become lighter and machine elements like aircraft equipment and turbine blade require high strength due to this composite materials are mostly used to satisfy this need.

A material made up of at least two constituents is a composite material and it makes up a very broad and important class of engineering material. Most of the time, a strong and stiff component is present, often in elongated form, embedded in a softer constituent forming the matrix.

By making composite material the Strength, Stiffness, Fatigue life, Wear & Corrosion resistance, Thermal conductivity & Acoustical insulation, Attractiveness and Weight reduction properties of the constituent elements will be improved. There are many types of composite. Which is fibrous composite**,** laminated composite, particulate composite and any combination of the above three. And another way of composite classification is shown below (Edition, no date)

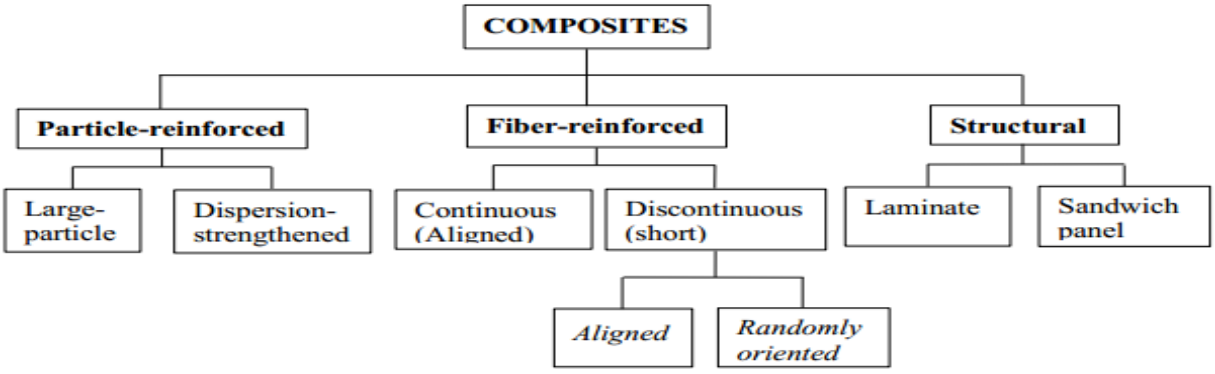

Figure 1-0-1 Types of composite materials

A laminated composite is a combination of resin and fiber mixed in an appropriate form. One of the exceptional properties of the composite laminate is that it has a high specific strength (strength to weight ratio). The properties of a laminated composite are a function of the resin and the fiber properties and geometry of the layers, which comprises size, distribution, orientation, shape, and quantity of fibers or particles. The resin gives a structure of a laminated material protects their surfaces and secures the load distribution by the fibers(Sudheer, Pradyoth and Somayaji, 2015).

Fiber-reinforced composites are usually made of a resin reinforced by short or long fiber material. Glass, carbon, aramid, silicon-carbide, and cellulose are the most widely used fiber for fiber-reinforced polymer because of their cost and excellent properties. From the many types of fiber material, fiberglass used for many applications because it is a lightweight and highly strong material(Yogesha, 2017). The main advantages of glass fibers are high tensile strength, low cost, high chemical resistance, and excellent insulating properties. (P.K. Mallik, 2007) The matrix material used for a fiber-reinforced polymer is a thermosetting plastic. Among different thermosetting material, epoxy resin and polyester are widely used due to their mechanical properties, environmental degradation, and availability('Guide to Composites', 2012). GFRP is a composite consist of either discontinuous or continuous glass fiber within a matrix material. Fiberglass applications now days are familiar in automotive, plastic pipes, storage containers, marine, industrial flooring, and aerospace(Borgaonkar et al, 2018). To decrease the vehicle weight and increase fuel efficiencies the transportation industries increase using GFRP. To keep natural resources and save energy, weight reduction has been the main attention of automobile manufacturers in the present situation. Design optimization, better manufacturing method and the introduction of improved material are the primary criteria for a weight reduction of a new automobile manufacturer. Suspension leaf spring is the main component for weight reduction in car manufacturing and it accounts for ten to twenty percent of the unsprung weight of the automobile. This helps in attaining the vehicle with better riding qualities.(Of *et al.*, 2018) For the same load capacity by appealing a composite light vehicle chassis there is a reduction in weight by more than 30% and the natural frequency is higher than the steel chassis by more than 35% and the composite chassis is stiffer than the steel chassis by 30 to 33.8 %. (Swamy, Lakshmaiah and Reddy, 2017)

Because of its specific properties laminated composite used as a fundamental structure and used in a complex working environment and it receives vibration, which may lead to crack on the structure. Any opening or defect in a composite material is a crack and it will be the cause of a rupture in any situation and the failure have two steps which are crack formation and crack propagation. Failure of engineering material is undesirable and causes the death of human and economic losses. Most of the time the causes of failures are misuse, improper material selection, processing and inadequate design of the component.

1.2. Statement of the problem

The Composite material is replacing conventional material for dynamically loaded structure in an automobile like leaf spring. Despite many applications of composite material for dynamically loaded structure, the introduction of a crack in a structure will cause catastrophic failure, If natural frequency equals the excitation frequency. Since natural frequency decrease by the presence of a crack.

The increased use of laminated composite for the structure under dynamic load increases the requirement of vibration analysis. The research intended for the design of a lightweight vehicle. So, studying the vibration of cracked GFRP will be a great benefit in the development of lightweight vehicles. In this research a new free vibration analysis especially the natural frequency of cracked GFRP to be conducted analytically, numerically and experimentally.

1.3. Objective

1.3.1. General Objective

The main objective of this paper is to study the free vibration, particularly the natural frequency of edge cracked glass fiber reinforced polymer (GFRP) laminate.

1.3.2. Specific objective

- To study the effect of crack depth on the natural frequency of the GFRP laminate.
- To study the effect of crack location on the natural frequency of the GFRP laminate.

1.4. Scope

Analytical and Numerical analysis was done to see the effect of crack location, and crack depth on the vibration characteristics of the laminate and experimental studies were conducted to validate the result. The numerical analysis was conducted by using ABAQUS 2017 software and experiment were performed using accelerometer ACC 103 and DAQ

USB NI-6009. Unidirectional and quasi-isotropic laminate for the experimental analysis was prepared by using a vacuum-assisted hand layup method. The specimens were prepared according to ASTM E756 standard.

1.5. Significant of the research

The focus of today's vehicle manufacturer is the reduction of weight to conserve natural resources and save energy. Weight reduction can be attained primally by the introduction of new material, design optimization, and better manufacturing process. So, studying the vibration properties of composite material have the following advantage

- Composite material replaces conventional material with reduced weight and reduction of weight conserve resources and save energy.
- Manufacturing of composite material is easy as compared with conventional material.

1.6. Paper organization

The first chapter is an introduction part. Which describes the general terms and concepts presented in the study and it includes the statement of the problem and the objectives of the research. The second chapter is the literature review part. In this chapter different related papers reviewed and some gaps identified. The third chapter contains the material, method, and methodology. In this chapter the materials used in the research describes and the three methods discussed, and the methodology presented. The fourth chapter states the result and discussion part. in the last chapter, chapter five conclusion, and recommendation made for the paper.

Chapter Two

2. Literature Review

2.1. Introduction

There are researches on vibration analysis of cracked laminated composite material and different works of literature on free vibration analysis of composite material using different methods. since composite material is the future and the current engineering material studying the dynamic properties of composite material with different fiber arrangement and aspect ratio and the effect of edge crack on the dynamic properties of the structure is a concern in the analysis of composite material

2.2. Related works

Vibration analysis of woven glass fiber and epoxy matrix composite plate was done by (Ratnaparkhi and Sarnobat, 2013) in this study experiment were conducted for free-free boundary conditions using different parameters like fiber orientation and aspect ratio.

Many researchers studied the effect of crack on the vibration properties of a structural beam. A crack in the material will decrease the natural frequency.

(Gowda, 2018) analyze the consequence of crack on the vibration of a cantilever beam made of different materials. Besides the type of material, the natural frequency decreases due to the crack even if the natural frequency and the change of the frequency is different for different materials.

(Barad et al, 2013) model the crack as rotational spring and analyze the effect of crack location and crack size on natural frequency. The crack depth and location greatly disturb the natural frequency. A crack near the fixed end has a significant effect and reducing the natural frequency than a crack of the same size at the free end. In this study experiments were did by introducing crack using wire cut electro-discharge machining and the natural frequency measured using LMS make FFT analyzer. (Sahu and Das, 2020) using first-order shear deformation theory analyze the effect of transverse multiple cracks on woven/glass epoxy composite with different boundary types.

Different methods used to study the natural frequency of composite material. Anew higher-order finite element model was proposed for free vibration study of laminated composite and sandwich plates (Belarbi *et al.*, 2017). The result compared with different literature

and showed good accuracy. (Kahya *et al.*, 2019) did a finite element model for free vibration examination of laminated composite beam with multiple open edge cracks and its experimental validation based on a first-order shear deformation theory. The model they used can capable of considering material elastic coupling among twisting, extension, and bending deformations and also the Poisson's effect and they conclude that the model provides a quick and simple way to determine the mode shape and natural frequency of the cracked laminate structure (Heydari et al, 2014) studied forced flexural vibration of cracked Timoshenko beam and use a continuous bilinear model for the displacement field and the equation of motion derived using Hamilton's principle. From the analysis, the result showed that the highest crack depth ratio has the highest natural frequency change and the result of crack location on change in natural frequency depends on the crack position relative to the nodes and the anti-nodes of the corresponding mode shape. As the number of layers increases the natural frequency also increases. (Chavan and Joshi, 2015) study the effect of the number of layers on the natural frequency with analytical, numerical and experimental analysis, in all the three methods the result indicated the natural frequency increase as the number of layer increase and the change in the aspect ratio change the natural frequency.

The vibration characteristics of the cracked composite beam depend not only on the crack depth but also depends on the fiber arrangement. (Krawczuk et al, 1997) study the modeling and vibration analysis of a cantilever composite beam with transverse open crack and from the analysis, the change in natural frequency strongly depends on the volume fraction and the angle of the fibers. (Kim *et al.*, 2019) investigated the natural frequency greatly affected by the location of the crack of a cracked laminated beam with a constant fiber angle. If the fiber angle increases from 0 to 45 the natural frequency of the cracked laminated beam decrease meaningfully with increasing the crack depth. For a fiber angle changes from 45 to 90, the reduction in the natural frequency of the cracked composite beam is little by little. The fiber orientation and boundary fixation of the composite laminated beam have a significant influence on the dynamic properties of the composite laminated beam dependent on the type of fiber and matrix material. (Ghoneam, 1995) investigate the dynamic properties of the laminated beam with various fiber arrangments with crack and without crack.

A crack on a beam introduces local flexibility, flexibility is the function of the crack depth. This flexibility changes the dynamic properties of the composite material, from a change in dynamic properties the crack depth and crack location can be identified. Identification of crack in a structure is a critical aspect for decision making about repair and replacement of the part. (Jassim *et al.*, 2013) reviewed the vibration occurrence of a cantilever beam. (Patil et al, 2016) studied free vibration of cracked and uncracked beam to identify the crack location and crack depth. (Aspragathos, 2016) analyze the effect of cracks on the dynamic properties of cracked beams and the identification of the crack location and crack depth in a cantilever beam from the vibration mode.

2.3. Modeling of cracked laminated beam

When a crack introduces in a material the local flexibility changed and this change can be modeled as the inverse of the flexibility coefficient. (Kim *et al.*, 2019) models the local flexibility at the crack with different spring in this study first-order shear deformation theory was used to study the vibration of a cracked composite laminate. The cracked part model using three springs to indicate the axial, bending and shear effect on the vibration properties. The model they used for the analysis were presented in the figure below.

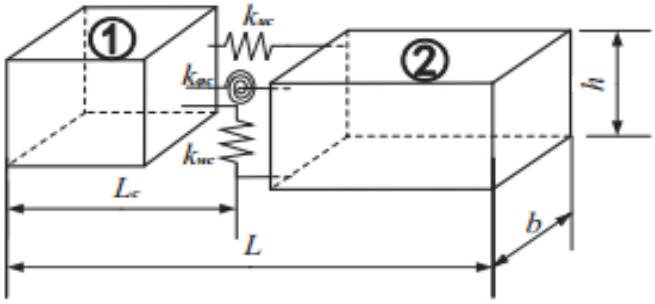

Figure 2-1 Modeling of a crack composite beam by first-order shear deformation theory

(Shaat *et al.*, 2016) developed a size-dependent Euler Bernoulli beam to study the vibration properties of cracked nanobeam material and model the crack as rotational spring.

2.4. Literature Gap

The review of related work showed that a crack in a composite structure changes the natural frequency of composite material and different research conducted the effect of crack size and crack location on vibration properties, specifically the natural frequency of composite material. Most of the literature was numerical and used woven type fiber as reinforced

material. Limited work was done by the experimental method (Das, 2018) reported in his literature only one paper was done for experimental vibration analysis of a straight composite beam. Some literature has studied the effect of crack on the vibration properties of composite material. In this paper, ABAQUS software was used for numerical analysis. Because ABAQUS software has a good result with a small percent error with the experimental analysis for composite material. (Degefe, 2015)

2.5. Conclusion

Crack in a structure decreases the stiffness of the material and the decrease in the stiffness of changes the dynamic properties especially the natural frequency. The effect of crack on the change of natural frequency depends on the geometry of the crack which is the depth of the crack and the location of the crack.

For different materials, the effect of crack on the natural frequency was different and in the case of composite material in addition to the crack depth and crack location the change of natural frequency depends on the fiber orientation and aspect ratio. Studying the effect of a crack in a structure can be used for structural health monitoring by identifying the size and location of the crack

Chapter Three

3. Material and Method

3.1. Materials

In this research unidirectional E glass fiber and epoxy with its hardener used for the preparation of the composite material. Unidirectional E glass fiber is obtained from Dejen Aviation, Bishoftu, Ethiopia. Whereas epoxy and its hardener obtained from the local market.

3.1.1. Glass fiber

Fiberglass is amongst the most multipurpose industrial materials known today. There are two classes of glass fiber which are premium special-purpose fiber and general-purpose, low-cost fiber. More than ninety percent of all fiberglass is under general-purpose products, and all fiberglass resulting from compositions containing silica. These fibers are known by the name E-glass fiber. E glass fiber is used as reinforcement material because it has good electrical insulator characteristics, cheap in price, higher mechanical strength than other glass-fiber types and low susceptibility to moisture. There are many types of E glass fiber. Which is unidirectional glass fiber, continuous glass fiber and chopped glass fiber. From the types of E glass fiber listed above unidirectional glass fiber is used in this paper. Unidirectional glass fiber has some good mechanical properties as compared to the other fiber type and most of the time unidirectional fiberglass used for the mechanical parts manufacturing.

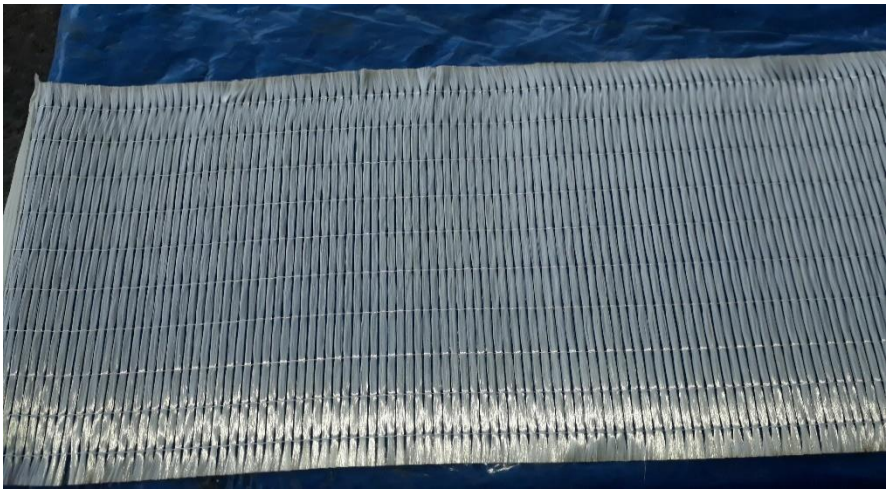

Figure 3-1 Unidirectional E Glass fiber

3.1.2. **Epoxy**

Epoxy is the matrix material used for this paper. Due to their mechanical properties, environmental degradation and its availability lead exclusive use for nowadays composite manufacturing. Its adhesive properties, and resistance to water, degradation makes epoxy resin ideal use for different applications. Epoxy 501 was used for this research. Epoxy resins are easily and quickly cured at any temperature from 5 °C to 150 °C, depending on the choice of curing agent. Epoxy resin has low shrinkage property during curing, which reduces internal stress and fabric print-through(‘Guide to Composites’, 2012).

3.1.3. Hardener

Epoxy resin requires a hardener to initiate curing and it is also used as a catalyst. The final characteristics of the composite will be determined by the selection and combination of the epoxy and the hardener. The ratio of epoxy resin to hardener used for this study was based on their masses. In general, the ratio is calculated based on curing time and the manufacturing guideline. The minimum curing time that occurs at the ratio of hardener to epoxy is 1:10. Finally, this proper amount of epoxy & hardener is mixed and stirred for a few minutes using in stick material.

3.2. Laminate design and composite plies

The properties of composite material depend on, the properties of the fiber and resin, the ratio of fiber to resin in the composite (fiber volume fraction), the geometry and orientation of the fibers in the composite. Plies in composite materials are substructures of the composite laminate and most of the time they are considered as prepreg (fiber pre-impregnated with partly cured resin) form. Composite laminate is formed by stacking different plies.

Fiber orientation

The arrangement or orientation of the fibers relative to one another [3] Fiber orientations of the composite material also has a high impact on modal density. So, a suitable material can be used for a certain application considering the vibrational properties of the material to eliminate the failure of the system.[6]

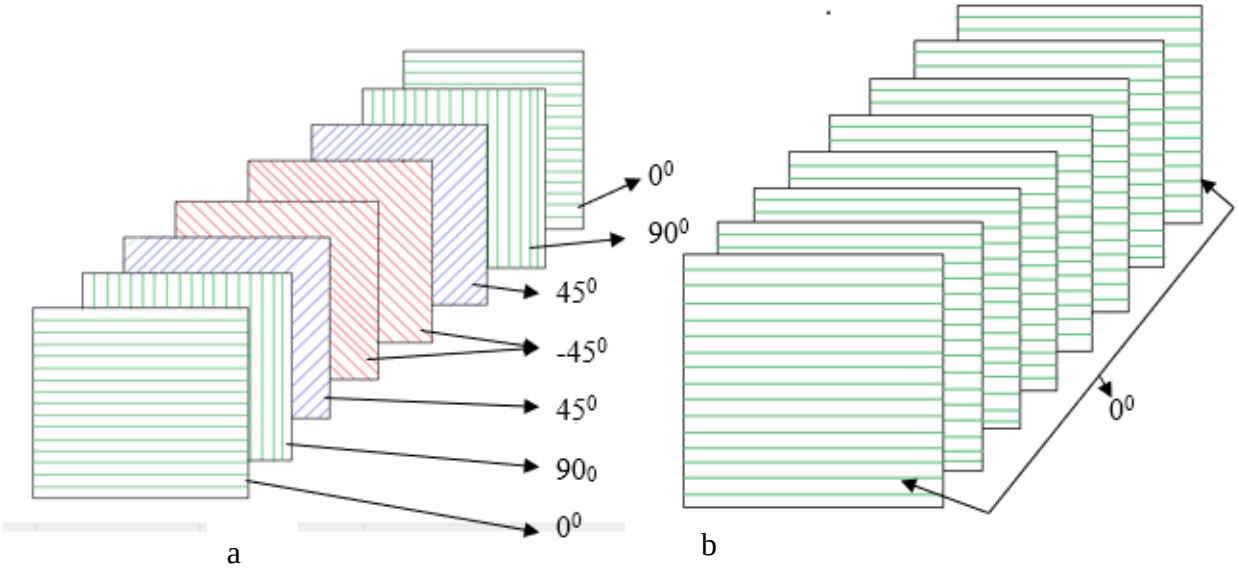

Figure 3-2 Lamina orientation a) quasi-isotropic lamina b) unidirectional lamina

3.3. Volume contents of the composite

The properties of composite material depend on the fraction of the fiber and the matrix material. So, in the analysis of composite material determining the volume fraction is a critical task. Determine the volume fraction of the composite are used for

- The preparation composite laminate and
- Numerical analysis

Fiber and matrix weight fraction

$$fiber\ wiegth\ fraction = \frac{weight\ of\ fiber}{total\ weight}$$

$$wf = \frac{wf}{w_f + w_m}$$

$$matrix\ weight\ fraction = \frac{weight\ of\ matrix}{total\ weight}$$

$$w_m = \frac{w_m}{w_{f+w_m}}$$

$$w_c = w_f + w_m$$

$$w_f + w_m = 1 \qquad (3.1)$$

Fiber and matrix volume fraction

$$v_f = \frac{w_f}{\rho_f}$$

$$v_m = \frac{w_m}{\rho_m}$$

$$v_c = v_f + v_m$$

$$Fiber\ volume\ fraction = \frac{volume\ of\ fiber}{total\ volume} = v_f = \frac{v_f}{v_c} = \frac{v_f}{v_f + v_m}$$

$$Matrix\ volume\ fraction = \frac{volume\ of\ matrix}{total\ volume}\ v_m = \frac{v_m}{v_c} = \frac{v_m}{v_f + v_m}$$

$$V_f = \frac{w_f + \rho_m}{w_f * \rho_m + w_m * \rho_f}$$

$$V_m = \frac{w_m + \rho_f}{w_f * \rho_m + w_m * \rho_f}$$

$$V_f + V_m = 1 \qquad (3.2)$$

The mass density of ply

$$\rho = \frac{total\ weight}{total\ volume} = \frac{weight\ of\ fiber + weight\ of\ matrix}{total\ volume}$$

$$= \frac{volume\ of\ fiber}{total\ volume}\rho_f + \frac{volume\ of\ matrix}{total\ volume}\rho_m$$

$$\rho = \rho_f * v_f + \rho_m * v_m \qquad (3.3)$$

Ply thickness h

$$h = \frac{total\ volume}{1(m^2)} = \frac{w_f}{v_f * \rho_f} \qquad (3.4)$$

where

Wf: the weight of Fiber (g) Wm: the weight of Matrix (g)

Wc: the weight of composite specimen (g) ρf: Density of Fiber (g/cc)

ρm: Density of Matrix (g/cc) Ply thickness (mm)

WF= Fiber weight fraction WM= matrix weight fraction

Vf: Volume of fibers, (cm3) Vm: Volume of the matrix, (cm3)

Vc: Volume of Composite specimen (cm3) VF: Fibers Volume fraction

VM: Matrix Volume fraction

From the literature review, the optimum fiber volume fraction is found for 40% to 60%, and the best volume fraction for glass fiber and epoxy material is 50% fiber volume fraction (Mr. Vishal S. Jagadale and PG, 2016). In this paper, the effect of crack location, and crack size for unidirectional and quasi-isotropic lamina was done for 50% percent fiber volume fraction.

For fifty percent fiber volume fraction, the mass density of the ply will be calculated as follow.

For a specimen prepared with (200x300x3) dimension in millimeter

The total volume of the ply is $V_t = 300 * 300 * 5 = 180$cc

The volume of the fiber $V_f = vf * Vt$=0.5*180=90cc

The volume of the matrix $V_m = vm * Vt$=0.5*180=90cc

Weight of the fiber $w_f = V_f * \rho_f = 90 * 2.6$=234g

Weight of the matrix $w_m = V_m * \rho_m = 225 * 1.2$=108g

Total weight is $w = 234 + 108 = 342$g

The mass density of ply

$$\rho = \frac{total\ weight}{total\ volume} = \frac{total\ weight}{total\ volume} = \frac{342}{180} = 1.9\,{}^{g}/_{cc}$$

Or using

$$\rho = \rho_f * v_f + \rho_m * v_m = 2.6 * 0.5 + 1.2 * 0.5 = 1.9\,{}^{g}/_{cc}$$

3.4. Elastic properties

Factors that determine the properties of composite materials are laminate thickness, fiber orientation, and fiber volume fraction or fiber weight fraction.

Different methods were used to analyze the mechanical properties of composite materials Which are analytical, numerical and experimental methods. The properties of composite material vary due to the types of fiber, polymer material, and fiber arrangements and as in the literature, the vibration properties of the cracked beam depend on the crack location and the crack depth.

Rule of mixture; It is the simplest method to determine the elastic properties for unidirectional composite material. Using this method, the properties of the composite material can be determined from the values of the fiber and the matrix.

Longitudinal properties

$$E_1 = E_f V_f + E_m(1 - V_f) \quad (3.5)$$

$$V_{12} = v_f V_f + v_m V_f \quad (3.6)$$

Transverse properties

$$E_2 = \frac{E_m E_f}{E_m V_f + E_f V_m} \quad (3.7)$$

$$v_{21} = \frac{v_{12}}{E_1} E_2 \quad (3.8)$$

Shear properties

$$G = \frac{E}{2(1+v)} \quad (3.9)$$

$$G_{12} = \frac{G_f G_m}{G_m V_f + G_f(1 - V_f)} \quad (3.10)$$

Using the above method, the elastic properties of the composite can be calculated from the properties of the constituent element given as follow [4]

Table 1 Elastic properties of constitute elements

Elastic properties	Epoxy resin	E-Glass
Young's modulus E in GPa	3.45	73.1
Poisson's ratio v	0.35	0.22
Shear modulus G in GPa	1.28	29.95
Density g/cc	1.2	2.6

Longitudinal properties

$$E_1 = E_f V_f + E_m v_m$$

$$E_1 = 73.1 * 0.5 + 3.45 * 0.5 = 38.275$$

The longitudinal properties for quasi-isotropic fiber laminate are different from the unidirectional fiber arrangement the longitudinal properties for the quasi-isotropic lamina is calculated as follows(Richardson, no date)

$$E_1 = \eta\theta E_f V_f + E_m v_m$$

Where ηθ =0.375 for quasi isotropic fiber orientation

$$E_1 = 0.375 * 0.5 * 73.1 + 0.5 * 3.45 = 15.43$$

$$V_{12} = v_f V_f + v_m V_f$$

$$V_{12} = 0.22 * 0.5 + 0.35 * 0.5 = 0.285$$

Transverse properties

$$E_2 = \frac{E_m E_f}{E_m V_f + E_f V_m}$$

$$E_2 = \frac{3.45 * 73.1}{3.45 * 0.5 + 73.1 * 0.5} = 6.589$$

$$v_{21} = \frac{v_{12}}{E_1} E_2$$

$$v_{21} = \frac{0.285}{38.275} * 6.589 = 0.05$$

Shear properties

$$G = \frac{E}{2(1+v)}$$

For the fiberglass

$$G = \frac{73.1}{2(1+0.22)} = 29.95$$

For the epoxy rein

$$G = \frac{3.45}{2(1+0.35)} = 1.28$$

Shera properties for the composite

$$G_{12} = \frac{G_f G_m}{G_m V_f + G_f (1 - V_f)}$$

$$G_{12} = \frac{29.95 * 1.28}{1.28 * 0.5 + 29.95 * 0.5} = 2.455$$

$$G_{23} = \frac{E_{22}}{2(1+v_{23})}$$

$$v_{23} = v_{21} = 0.05$$

$$G_{23} = \frac{6.589}{2(1+0.05)} = 3.14$$

3.5. Stiffness matrix

The lamina elastic coefficients ${Q_{ij}}^k$ can be obtained from the material properties of the kth orthotropic lamina layer.

$$Q_{11}{}^{k} = \frac{E1^{k}}{1-\mu^{k}{}_{12}\mu^{k}{}_{21}},\quad Q_{12}{}^{k} = \frac{\mu^{k}{}_{12}E2^{k}}{1-\mu^{k}{}_{12}\mu^{k}{}_{21}}, Q_{22}{}^{k} = \frac{E2^{k}}{1-\mu^{k}{}_{12}\mu^{k}{}_{21}}, Q_{44}{}^{k} = G^{k}{}_{23}$$

$$Q_{55}{}^{k} = G^{k}{}_{13}, Q_{66}{}^{k} = G^{k}{}_{12} \tag{3.11}$$

3.6. ABD matrix of the composite lamina

$$A_{ij} = \sum_{k=1}^{Nk}\left[Q_{ij}{}^{-k}\right]_{k}(Z_{K+1} - Z_{k}) \tag{3.12}$$

$$B_{ij} = \frac{1}{2}\sum_{k=1}^{Nk}\left[Q_{ij}{}^{-k}\right]_{k}(Z_{K+1}{}^{2} - Z_{k}{}^{2}) \tag{3.13}$$

$$D_{ij} = \frac{1}{3}\sum_{k=1}^{Nk}\left[Q_{ij}{}^{-k}\right]_{k}(Z_{K+1}{}^{3} - Z_{k}{}^{3}) \tag{3.14}$$

Where

$$Q_{11}{}^{-k} = Q_{11}{}^{k}m^{4} + 2\left(Q_{12}{}^{k} + 2Q_{66}{}^{k}\right)m^{2}n^{2} + Q_{22}{}^{k}n^{2} \tag{3.15a}$$

$$Q_{12}{}^{-k} = \left(Q_{11}{}^{k} + Q_{22}{}^{k} - 4Q_{66}{}^{k}\right)m^{2}n^{2} + Q_{12}{}^{k}(m^{2}+n^{2}) \tag{3.15b}$$

$$Q_{22}{}^{-k} = Q_{11}{}^{k}n^{4} + 2\left(Q_{12}{}^{k} + 2Q_{66}{}^{k}\right)m^{2}n^{2} + Q_{22}{}^{k}m^{4} \tag{3.15c}$$

$$Q_{16}{}^{-k} = \left(Q_{11}{}^{k} - Q_{12}{}^{k} - 2Q_{66}{}^{k}\right)m^{3}n + \left(Q_{12}{}^{k} - Q_{22}{}^{k} + 2Q_{66}{}^{k}\right)mn^{3} \tag{3.15d}$$

$$Q_{26}{}^{-k} = \left(Q_{11}{}^{k} - Q_{12}{}^{k} - 2Q_{66}{}^{k}\right)n^{3}m + \left(Q_{12}{}^{k} - Q_{22}{}^{k} + 2Q_{66}{}^{k}\right)nm^{3} \tag{3.15e}$$

$$Q^{-k}{}_{66} = \left(Q^{k}{}_{11} + Q^{k}{}_{22} - 2Q^{k}{}_{12} - 2Q^{k}{}_{66}\right)m^{2}n^{2} + Q^{k}{}_{66}(m^{4} + n^{4}) \tag{3.15f}$$

$$Q_{44}{}^{-k} = Q_{44}{}^{k}m^{2} + Q_{55}{}^{k}n^{2} \tag{3.15g}$$

$$Q_{45}{}^{-k} = (Q_{55}{}^{k} - Q_{44}{}^{k})mn \tag{3.15h}$$

$$Q_{55}{}^{-k} = Q_{55}{}^{k}m^{2} + Q_{44}{}^{k}n^{2} \tag{3.15i}$$

Where

$$m = cos\alpha^{k}{}_{fiber}\, n = sin\alpha^{k}{}_{fiber} \tag{3.16}$$

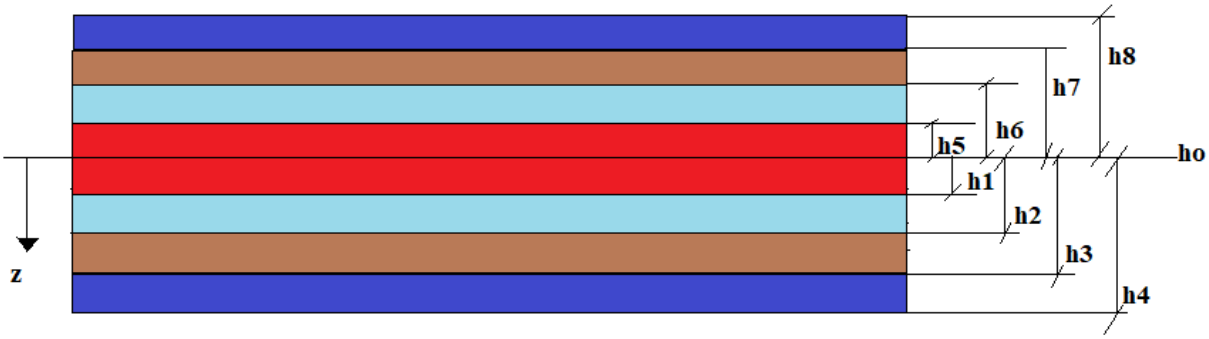

Figure 3-3 Symmetric layers of composite plate

Where [A] = extensional stiffness matrix for the laminate (unit: N/m)

$$[A]=\begin{bmatrix} A_{11} & A_{12} & A_{16} \\ A_{21} & A_{22} & A_{26} \\ A_{16} & A_{26} & A_{66} \end{bmatrix}$$

$$Amn = \left((\bar{Q}mn)1(h4-h3) + (\bar{Q}mn)2(h3-h2) + (\bar{Q}mn)3(h2-h1)\right) + \left((\bar{Q}mn)4(h1-h0) + (\bar{Q}mn)5\left(h0-(-h5)\right)\right) + (\bar{Q}mn)\,6(-h5-(-h6)) + (\bar{Q}mn)\,7(-h6-(-h7)) + (\bar{Q}mn)\,8(-h7-(-h8)))$$

[B]= coupling stiffness matrix for the laminate (unit: N)

$$[B]=\begin{bmatrix} B_{11} & B_{12} & B_{16} \\ B_{12} & B_{22} & B_{26} \\ B_{16} & B_{26} & B_{66} \end{bmatrix}$$

$$Bmn = 1/2((\bar{Q}mn)1(h42-h32) + (\bar{Q}mn)2(h32-h22) + ((\bar{Q}mn)3(h22-h12) + (\bar{Q}mn)4(h12-h02)) + ((\bar{Q}mn)5(h02-h52) + (\bar{Q}mn)6(h52-h62)) + ((\bar{Q}mn)\,7(h62-h72) + (\bar{Q}mn)\,8(h72-h82)))$$

The [Bij] matrix is called as the extension-bending coupling stiffness matrix. [Bij] becomes zero for symmetric lamina because the contribution of the lamina to a particular term of the B matrix is given by the product of the corresponding term in the $\bar{Q}$ matrix and the difference of the squares of z coordinates of the top and bottom surface of each ply. The contribution of a lamina above the geometric mid-plane can be eliminated by placing an identical lamina below the mid-plane. (Flight, 2019) (Raton, 1995)

[D] = bending stiffness matrix for the laminate (unit: N m or lb-in.)

$$[D]=\begin{bmatrix} D_{11} & D_{12} & D_{16} \\ D_{12} & D_{22} & D_{26} \\ D_{16} & D_{26} & D_{66} \end{bmatrix}$$

$$Dmn = (1/3\,((\bar{Q}mn)1(h43-h33) + (\bar{Q}mn)2(h33-h23)) + (+(\bar{Q}mn)3(h23-h13) + (\bar{Q}mn)4(h13-h03)) + (+(\bar{Q}mn)5(h03-(-h5)3) + (\bar{Q}mn)6(-h53-(-h6)3)) + (+(\bar{Q}mn)7(-h63-(-h7)3)) + ((\bar{Q}mn)\,8(-h73-(-h8)3))$$

3.7. Description of cracked laminated beam

A crack will be located in Lc distance from the crack. The length of the crack is L, the width of the crack is b and the thickness denoted by h. a cartesian coordinate system is used, on which the longitudinal direction is the x-axis which is, the length direction.

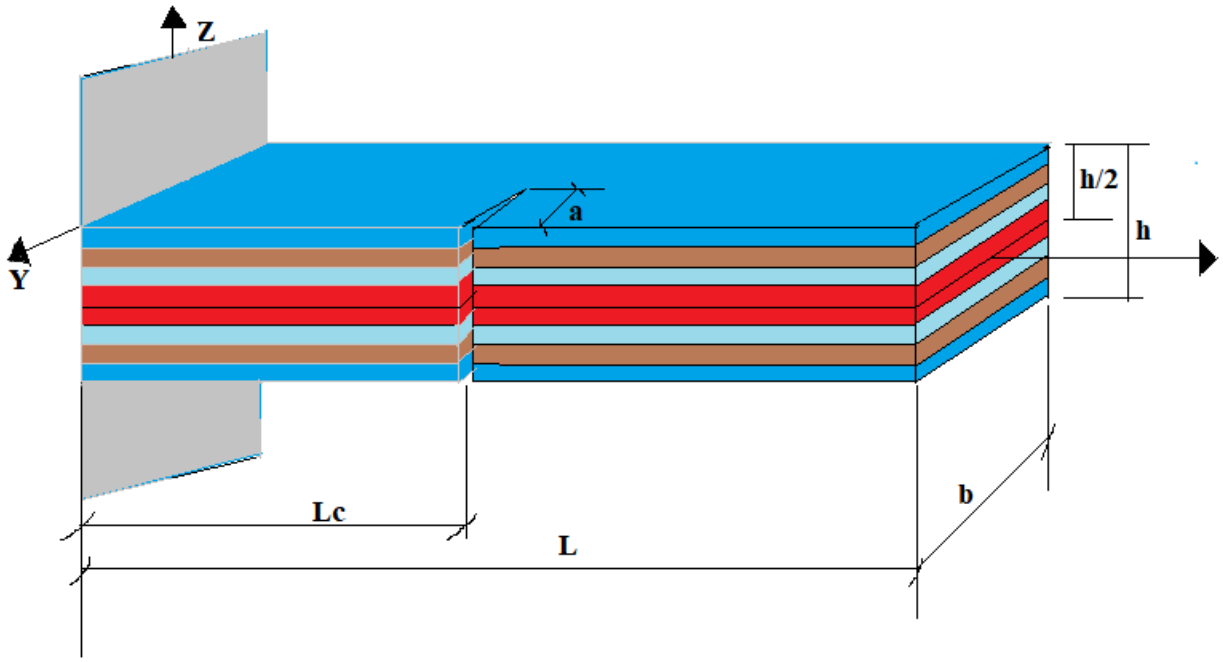

Figure 3-4 Geometrical description of cracked laminated beam

3.8. Methods

The research uses analytical, numerical and experimental methods.

3.8.1. Analytical Method

The properties of the composite material were calculated in section 3.4. The elastic properties of the matrix material and E glass are shown in table 1. From reference [4], the young's modulus and the position ratio are calculated using the rule of the mixture were in good agreement with finite element analysis using ANSYS software with varying fiber volume fraction.

3.8.1.1. Vibration analysis of composite beam

The vibration analysis of the glass epoxy composite beam is the calculation of the natural frequency and damping properties of the material. In this study, first-order shear deformation theory (FSDT) was used. FSDT includes the effect of transverse shear deformation. A cantilever beam as shown in fig 3-4 is selected for analysis. In this study,

a beam with Eight layers and 180 mm length, 30 mm width and 3 mm thickness were used. The arrangement of the fiber is symmetric about the centroid.

The discontinuities at the crack model by a spring. Here a spring used to model the crack.

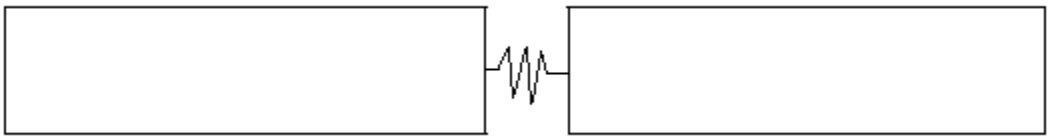

Figure 3-5 Modeling of cracked composite beam

Based on first-order shear deformation theory the displacement field for the beam is described in equation 3.17 and it is assumed that the deformation of the beam takes place in the x-z plane and also it is assumed that there is no warping effect. (Reddy, 1997)

$$\left.\begin{aligned} U(x,z,t) &= u(x,t) + z\varphi(x,t) \\ W(x,z,t) &= w(x,t) \end{aligned}\right\} \quad (3.17)$$

Where u and w represent the center-line displacement along x and z-direction of the beam and φ is an unknown function that represents a shear strain on the center-line of the beam. The strain displacement relations are given by(Sahu and Das, 2020)

$$\left.\begin{aligned} \varepsilon x &= \varepsilon x x^0 + kxx \\ \gamma xz &= \gamma xz^0 \end{aligned}\right\} \quad (3.18)$$

Where

$$\left.\begin{aligned} \varepsilon x x^0 &= \frac{\partial u}{\partial x} \\ kxx &= \frac{\partial \varphi}{\partial x}, \\ \gamma xz^0 &= \varphi + \frac{\partial w}{\partial x} \end{aligned}\right\} \quad (3.19)$$

3.8.1.2. Stress intensity factor of cracked composite plate

In this section, the methods for calculating stress intensity factors of cracked composite plates corresponding to generalized loading conditions is described.

The stress intensity factors of the three modes of fracture, which are opening, sliding and tearing types correspond to the generalized loading as shown in fig 3-6.

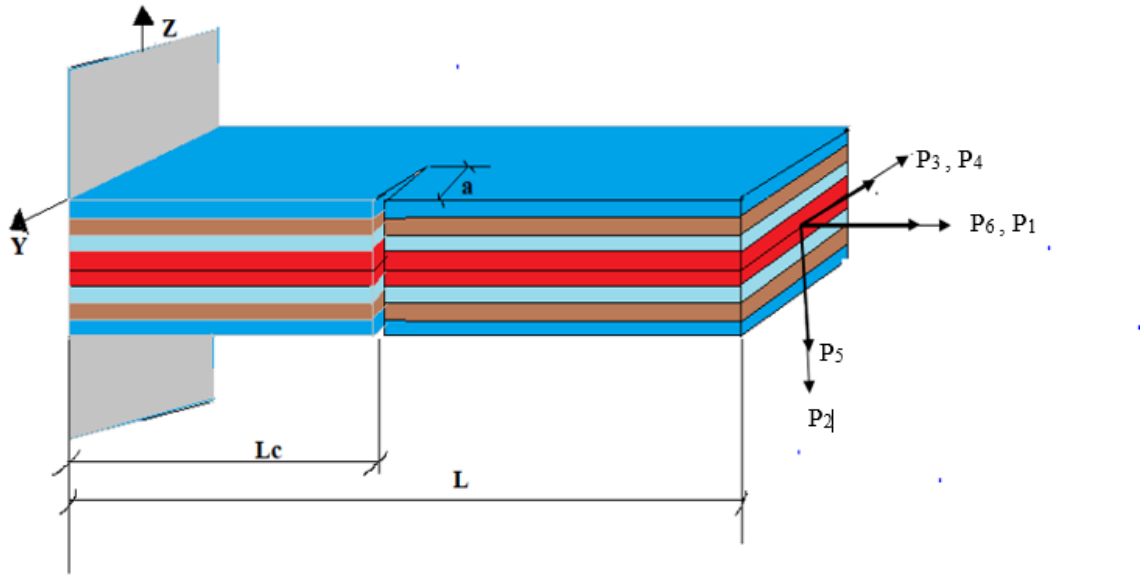

Figure 3-6 the cracked laminated beam under general loading condition

As shown in fig 3-6 the general loading condition indicated by an axial force P_1, shear force P_2 and P_3, bending moment P_4 and P_5 and torsional moment P_6.

The stress intensity factors *K*jn (*j* = I, II, III) of the composite plate cannot be taken in the same form as the stress intensity factors of anisotropic material in the same loading and geometry conditions. The stress intensity factors Kjn(j = I, II, III) of the fiber-reinforced composite beam can be expressed as.[20]

$$K_{jn} = \sigma_n\sqrt{\pi a}F_{jn}(a/h, \lambda^{\frac{1}{4}} L/h, \delta) \quad (3.20)$$

Where

σ_n is the stress

A is the crack depth

Fjn is the correction function according to the geometric shape of the plate.

λ and δ are dimensionless parameters taking into account the in-plane orthotropic and defined as functions of the elastic constants by

$$\lambda = E_{22}/E_{11} \quad (3.21)$$

$$\delta = \sqrt{E22E11/2G12} - \sqrt{\mu_{12}\mu_{21}} \quad (3.22)$$

where $\lambda^{\frac{1}{4}}$ L/h $\geq$ 2, the term related to $\lambda^{\frac{1}{4}}$ L/h is ignored. For a fiber-reinforced composite beam whose aspect(L/4) ratio greater than 4, it satisfies this condition, the stress intensity factor K_{jn} becomes.

$$K_{jn} = \sigma_n\sqrt{\pi a}F_{jn}(a/h)\ Y_j(\ \delta) \tag{3.23}$$

Where

$Y_j(\delta)$ is the correction function for anisotropic and

$F_{jn}((a/b)$ takes the same form as correction function in an isotropic material selected according to the geometry shape of the plate and loading acting on the beam.

The stress intensity factor of the unidirectional glass fiber reinforced composite beam is determined as follows.

$$\begin{gathered}
K_{I1} = \sigma_1\sqrt{\pi a}F_1(a/b)Y_1(\ \delta),\ \ \sigma_1 = \frac{P1}{bh} \\
K_{I4} = \sigma_4\sqrt{\pi a}\ Y_1(\ \delta)\ F_2(a/b),\ \ \sigma_4 = \frac{12P_4}{bh^3}z \\
K_{I5} = \sigma_5\sqrt{\pi a}\ Y_1(\ \delta)\ F_2(a/b),\ \ \sigma_4 = \frac{6P_4}{bh^2} \\
K_{I2} = K_{I3} = K_{I6} = 0 \\
K_{II3} = \sigma_1\sqrt{\pi a}\ Y_{II}(\ \delta)\ F_{II}(a/b),\ \ \sigma_1 = \frac{P_3}{bh} \\
K_{II1} = K_{II2} = K_{II4} = K_{II5} = K_{I6} = 0 \\
KIII2 = \sigma_2\sqrt{\pi a}\ Y_{III}(\ \delta)\ F_{III}(a/b),\ \ \sigma_2 = \frac{P_2}{bh} \\
KIII6 = \sigma_6\sqrt{\pi a}\ Y_{III}(\ \delta)\ F_{III}(a/b),\ \ \sigma_6 = \frac{24P_6\pi^3}{\pi^5bh^2-192h^3}\cos(\frac{\pi}{h}z) \\
K_{III1} = K_{III3} = K_{III5} = 0
\end{gathered} \tag{3.24}$$

Where

$$F_1(a/b) = \sqrt{\frac{2h}{\pi\Im}\tan\frac{\pi a}{2b}}\,\frac{0.752+2.02\left(\frac{a}{h}\right)+0.37\left(1-\sin\frac{\pi a}{2b}\right)^3}{\cos\frac{\pi a}{2b}}$$

$$F_2(a/b) = \sqrt{\frac{2h}{\pi\Im}\tan\frac{\pi a}{2b}}\,\frac{0.923+0.199\left(1-\sin\frac{\pi a}{2b}\right)^4}{\cos\frac{\pi a}{2b}}$$

$$F_{II}(a/b) = \frac{1.122-0.561\left(\frac{a}{b}\right)+0.085\left(\frac{a}{b}\right)^2+0.18\left(\frac{a}{b}\right)^3}{\sqrt{1-\left(\frac{a}{b}\right)}}$$

$$F_{III}(a/b) = \sqrt{\frac{2h}{\pi a}\tan\frac{\pi a}{2b}} \qquad (3.25)$$

And

$$Y_I(\delta) = 1+ 0.1(\delta-1) - 0.016(\delta-1)^2 + 0.002(\delta-1)^3,\ Y_{II}(\delta) = Y_{III}(\delta) = 1 \qquad (3.26)$$

3.8.1.3. Cracked composite beam modeling

At the crack section, the cracked beam is separated into two parts and a continuous condition at the connecting face is modeled by the inverse of the flexibility coefficient. The additional strain energy due to the existence of the crack can be expressed as(Kim *et al.*, 2019)

$$U_C = \int J(\xi)dA \qquad (3.27)$$

The flexibility coefficient which are functions of stress intensity factor and the crack shape can be expressed as.

$$c_{ij} = \frac{\partial wi}{\partial pi} = \frac{\partial^2 Uc}{\partial pipj} = \frac{\partial^2}{\partial pipj}\int J(\xi)dA \qquad (3.28)$$

For an existing stress intensity factor Kjn, the local flexibility matrix Cjn are expressed as

$$c_{ij} = \frac{\partial^2}{\partial pipj}\int_{-h/2}^{h/2}\int_0^a [D1(KI1+KI4+KI5)^2 + D2KII3^2 + D12(KI1+KI4+KI5)KII3 + D3(KIII2+KIII6)^2]\,d\xi\,dz \qquad (3.29)$$

For the composite under this study, there exist three independent variables which are the axial displacement, the vertical displacement and the rotational displacement of the cross-section. The corresponding flexibility matrix is given by

$$c_{ij} = \frac{\partial^2}{\partial pipj}\int_{-h/2}^{h/2}\int_0^a [D1(KI1+KI4)^2 + D3(KIII2)^2]\,d\xi\,dz \qquad (3.30)$$

when the orientation angle of the fiber in every layer is different, the coefficients D will be changed, so the flexibility matrix corresponding to the entire height of the cracked laminated beam can be written as

$$\left.\begin{aligned} c_{11} &= \frac{2\pi YI(\delta)^2}{b^2h^2}\sum_{k=1}^{n} D1k \int_{h1}^{hu}\int_{0}^{a} \xi F1^2(\xi/b)\, d\xi\, dz \\ c_{22} &= \frac{2\pi YIII(\delta)^2}{b^2h^2}\sum_{k=1}^{n} D3k \int_{h1}^{hu}\int_{0}^{a} \xi FIII^2(\xi/b)\, d\xi\, dz \\ c_{44} &= \frac{288\pi YI(\delta)^2}{b^2h^6}\sum_{k=1}^{n} D1k \int_{h1}^{hu}\int_{0}^{a} \xi F2^2(\xi/b)\, d\xi\, dz \end{aligned}\right\} \quad (3.31)$$

The connecting spring can be written as

$$k_{uc} = {c_{11}}^{-},\ k_{wc} = {c_{22}}^{-},\ k_{\phi c} = {c_{44}}^{-} \quad (3.32)$$

The spring force stored in the spring is expressed as

$$Kt = k_{uc} * u + k_{wc} * w + k_{\phi c} * \phi$$

$$\begin{bmatrix} Kuc & 0 & 0 \\ 0 & Kwc & 0 \\ 0 & 0 & K\phi c \end{bmatrix}\begin{bmatrix} Am \\ Cm \\ Bm \end{bmatrix} \quad (3.33)$$

The equation of motion using first-order shear deformation theory for uncracked beam given by

$$\left.\begin{aligned} \frac{\partial N}{\partial x} &= I_1\frac{\partial^2 u}{\partial t^2} + I_2\frac{\partial^2 \emptyset}{\partial t^2} - p_x \\ \frac{\partial M}{\partial x} &= I_2\frac{\partial^2 u}{\partial t^2} + I_3\frac{\partial^2 \emptyset}{\partial t^2} + Q \\ \frac{\partial Q}{\partial x} &= I_1\frac{\partial^2 \emptyset}{\partial t^2} - p_z \end{aligned}\right\} \quad (3.34)$$

$$u_0, w_0, \varphi_0 = \sum_{m=1}^{M}[A_m \cos(\alpha_m x), C_m \sin(\alpha_m x), B_m \cos(\alpha_m x)] \sin(\omega t) \quad (3.35)$$

Substituting Eq.3.35 in the equation of motion, Eq. 3.34 it becomes the following characteristics equation.

$$\begin{bmatrix} c11 & c12 & c13 \\ c21 & c22 & c23 \\ c31 & c32 & c33 \end{bmatrix}\begin{bmatrix} Am \\ Cm \\ Bm \end{bmatrix} + \omega^2\begin{bmatrix} I1 & 0 & I2 \\ 0 & -I1 & 0 \\ I2 & 0 & I3 \end{bmatrix}\begin{bmatrix} Am \\ Cm \\ Bm \end{bmatrix} + \begin{bmatrix} Pxm \\ -Pzm \\ 0 \end{bmatrix} = 0 \quad (3.36)$$

Where

$$\left.\begin{aligned} c_{11} = -{\alpha_m}^2 A_{11},\ c_{22} = {\alpha_m}^2 A_{55}, \\ c_{33} = -{\alpha_m}^2 D_{11} - A_{55},\ c_{31} = c_{13} = -{\alpha_m}^2 B_{11}, \\ c_{23} = c_{32} = {\alpha_m}^2 A_{55},\ c_{12} = c_{21} = 0 \end{aligned}\right\} \quad (3.37)$$

Combine equation 3.36 with equation 3.39 we get the general equation for the cracked composite beam

$$\begin{bmatrix} c11 & c12 & c13 \\ c21 & c22 & c23 \\ c31 & c32 & c33 \end{bmatrix}\begin{bmatrix} Am \\ Cm \\ Bm \end{bmatrix} - \begin{bmatrix} Kuc & 0 & 0 \\ 0 & Kwc & 0 \\ 0 & 0 & K\phi c \end{bmatrix}\begin{bmatrix} Am \\ Cm \\ Bm \end{bmatrix} + \omega^2 \begin{bmatrix} I1 & 0 & I2 \\ 0 & -I1 & 0 \\ I2 & 0 & I3 \end{bmatrix}\begin{bmatrix} Am \\ Cm \\ Bm \end{bmatrix} + \begin{bmatrix} Pxm \\ -Pzm \\ 0 \end{bmatrix} = 0 \quad (3.38)$$

3.8.2. Numerical Method

All the simulations and analyses were conducted using ABAQUS. As a general-purpose finite element analysis code, based on user and reference ABAQUS, it has been widely used in all industries and academics for solving engineering problems, including automotive, aerospace, defense, energy, and life sciences.

ABAQUS /CAE or ‘’Complete ABAQUS Environment ‘’ is a software application used for both modeling and analysis of mechanical components and assemblies (pre-processing) and visualizing the finite element analysis result.

3.8.2.1. Finite element modeling

The finite element simulation was based on the ASTM E756 standard. The dimensions of the specimen used were 180 mm length, 30 mm width, and 3 mm thickness. Each lamina had 0.375mm thickness. A cantilever beam was used for analysis**.**

Properties of the laminate

As calculated in section 3.4 using the rule of mixture the properties of the laminate are listed in table 2.

Table 2 Elastic properties of laminate

Material properties	Unidirectional	Quasi isotropic
Longitudinal modulus of elasticity (Gpa)	38.275	15.43
Transverse modulus of elasticity (Gpa)	6.589	6.589
Shera modulus of elasticity in XY plane (Gpa)	2.45	2.45
Shear modulus of elasticity in YZ plane (Gpa)	3.14	3.14
Passion ratio in XY plane	0.285	0.285
Passion ration in YZ plane	0.05	0.05

The numerical analysis was conducted in the following steps

- Part: modeling the structure with the specified dimension
- Properties; material properties, fiber arrangement, and section assignment
- Assembly: assemble different parts
- Step; this module is used to select the types of analysis performed
- Interaction; assigning cracks
- Load; apply any external force on the structure
- Mesh; discretizing the structure to the element size
- Optimization;
- Job; summit the given data for analysis
- Visualization; show different results
- Sketch; draw graphs from the result

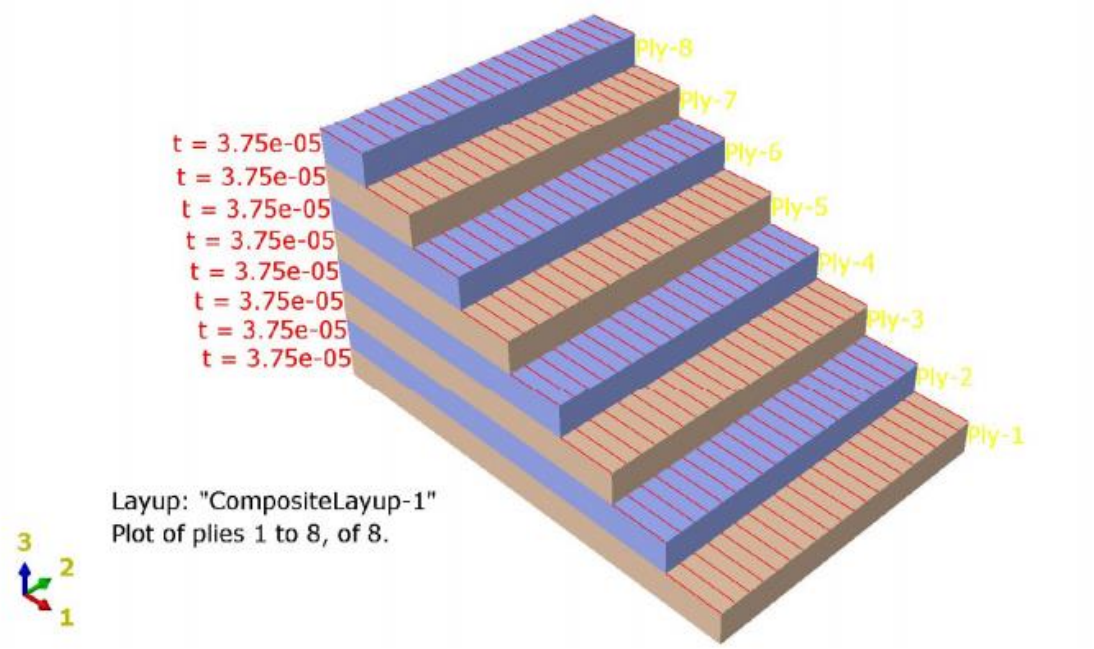

Figure 3-7 Ply stack plot for unidirectional lamina orientation

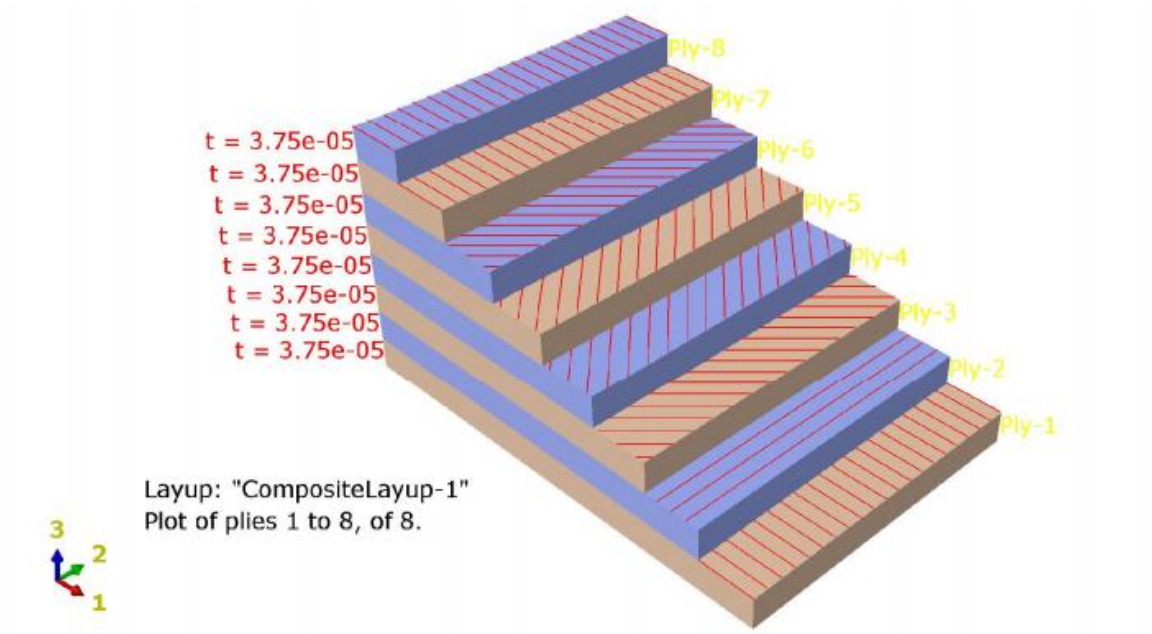

Figure 3-8 Ply stack plot for quasi-isotropic lamina orientation

3.8.2.2. Meshing

In this paper, a solid element C3D8R element was used and the same element number use for all the specimens.

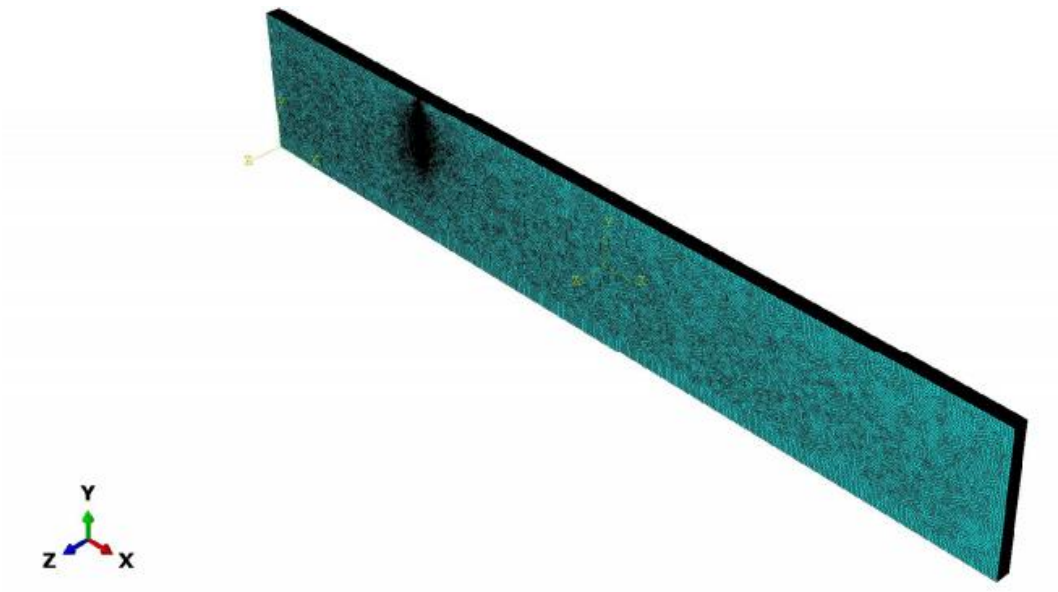

Figure 3-9 3D Mesh of Cracked beam

3.8.3. Experimental Method

3.8.3.1. Composite manufacturing

Hand layup assisted with vacuum bagging method

Vacuum impregnation is a process in which the resin to fiber wetting is assisted by a vacuum. The main purpose of the vacuum process is it removes the air which, is trapped inside the laminate, thus reducing the defect and improving the strength of the laminate. some of the advantages of the vacuum impregnation method are improving the strength of the laminates by reducing the defects, when compared with mould laminates it is a low-cost method and the density of the laminate is significantly lower than compression mould. The effects of the vacuum method on the reinforcements are good formability, good surface quality, high strength, and wear resistance. A vacuum bag is used to contain the vacuum generated by the pump and applied to the lay-up. The application of the vacuum bag is very critical. Bag porosity or punctures can result in a porous product.

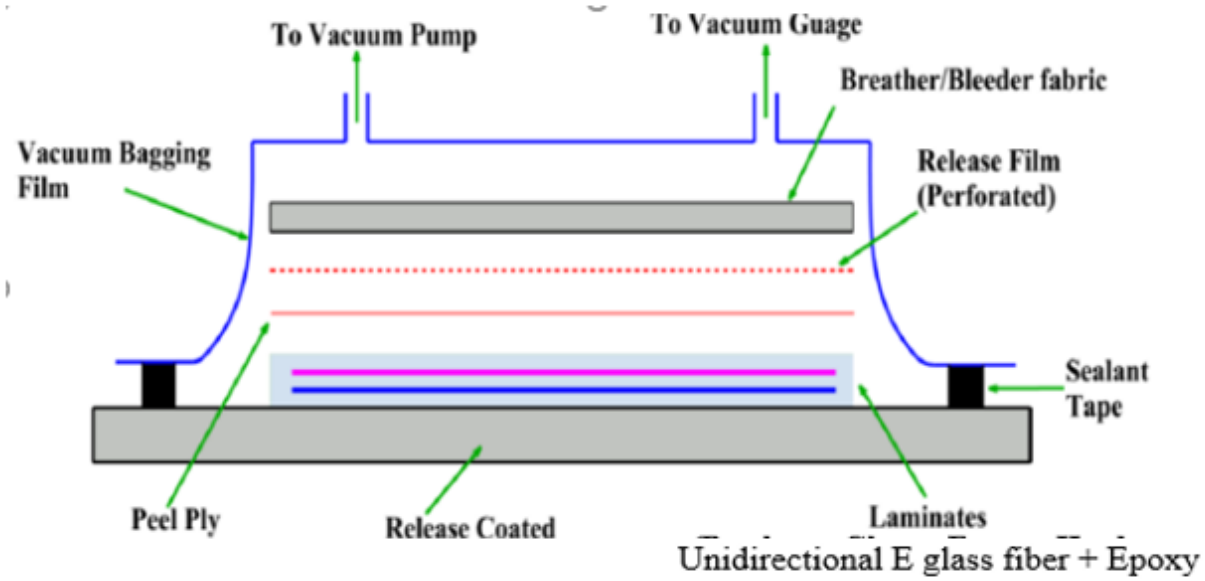

Figure 3-10 Hand layup assisted by vacuum bagging technique

3.8.3.2. Vacuum bagging equipment's

Vacuum pump

vacuum pumps are mechanically similar to air compressors but work in the opposite so that air is drawn from the closed system and exhausted to the atmosphere. The heart of a vacuum bagging system is the vacuum pump.

Figure 3-11 Vacuum pump

Release fabric (peel ply)

A smooth woven fabric used to separate the breather and the laminate. Excess epoxy can wick through the peel ply and be peeled off the laminate after the laminate cures.

Perforated film

It used in conjunction with the peel ply. This film helps to hold the resin in the laminate when high vacuum pressure is used with slow curing resin systems or thin laminates.

Breather material

The breather cloth allows air from all parts of the envelope to be drawn to the manifold by providing a slight air space between the bag and the laminate.

Vacuum bag

The vacuum bag in most cases forms half of the sealed envelope around the laminate.

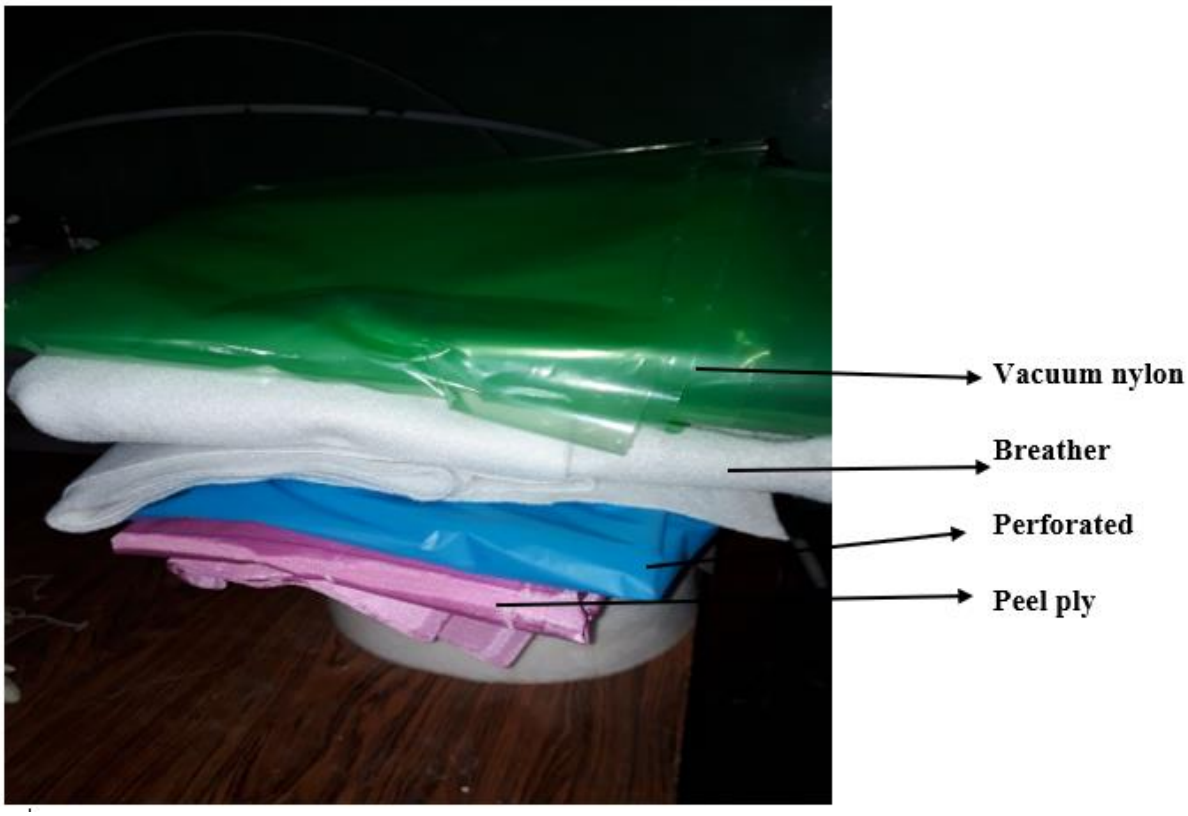

Figure 3-12 Hand layup assisted vacuum bagging indirect materials

Vacuum tape

it is used to provide a continuous seal between the mold and the bag around the perimeter of the mold. it also is used to seal the point where the manifold enters the bag and to repair leaks in the bag or plumbing.

Figure 3-13 Vacuum tape

Mould: The mould will have the shape of the product. In order to have a glossy or textured finish on the surface of the product, the mould surface also should have the respective finish **Release Film or Layer:** Since the resins used are highly adhesive, the product may get stuck to the mould. So, a proper releasing mechanism should be incorporated.

Figure 3-14 Release wax

Tools for hand lay-up

1. Weighing balance - to weigh the chemicals.
2. Brushes - to apply resin for both gel coat application and for lamination.
3. Rollers - to remove the air bubbles and also for applying resin.

3.8.3.3. Specimen preparation procedure

To manufacture the laminated composite an open flat aluminum mould was used. First, the surface of the mould was cleaned and a releasing agent wax was applied. Epoxy 501 with a ten percent hardener was used as a matrix material. Then, the resin was applied to each layer using a hand layup process. Unidirectional E glass fiber was cut in the required number of layers with specified sizes. After the completion of the hand layup process, the peel ply, transfer media, and breather were layer-up on the top of the laminate. to get a smooth surface finish a peel play is used to cover the laminate.

Vacuum nylon was used around the mold and sealed by using vacuum tape around the parameter of mould. Finally, the mould connected with the vacuum pump and the reservoir by using a vacuum hose. Then the mould was under vacuum at 0.9 atm for 8 hrs. and cured at room temperature for 72 hrs.

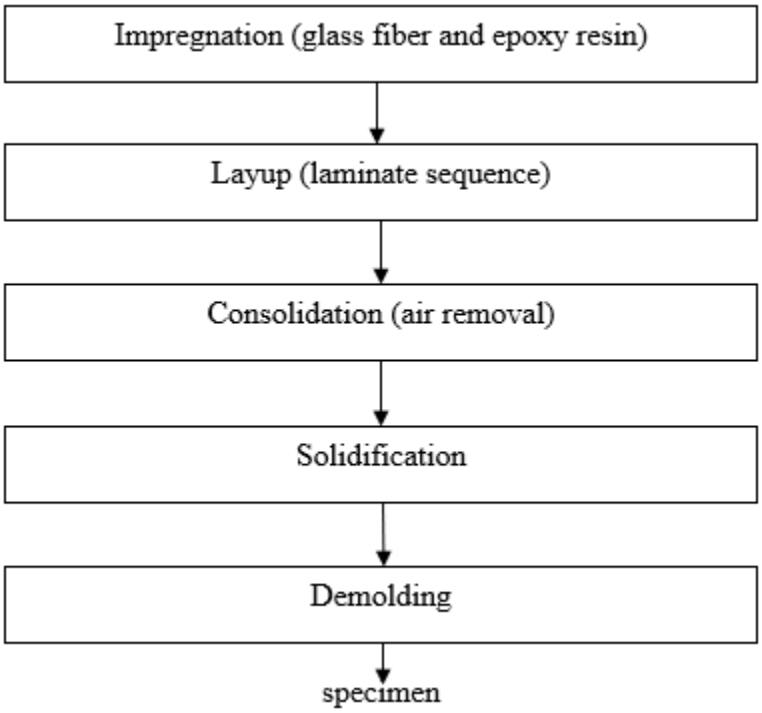

Figure 3-15 Composite manufacturing steps

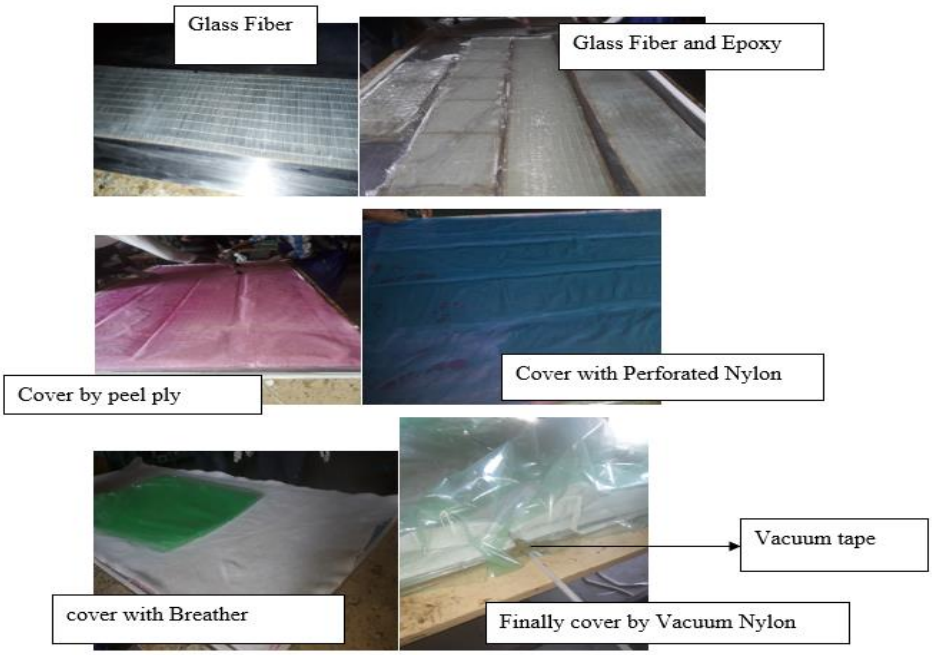

Figure 3-16 Composite manufacturing steps

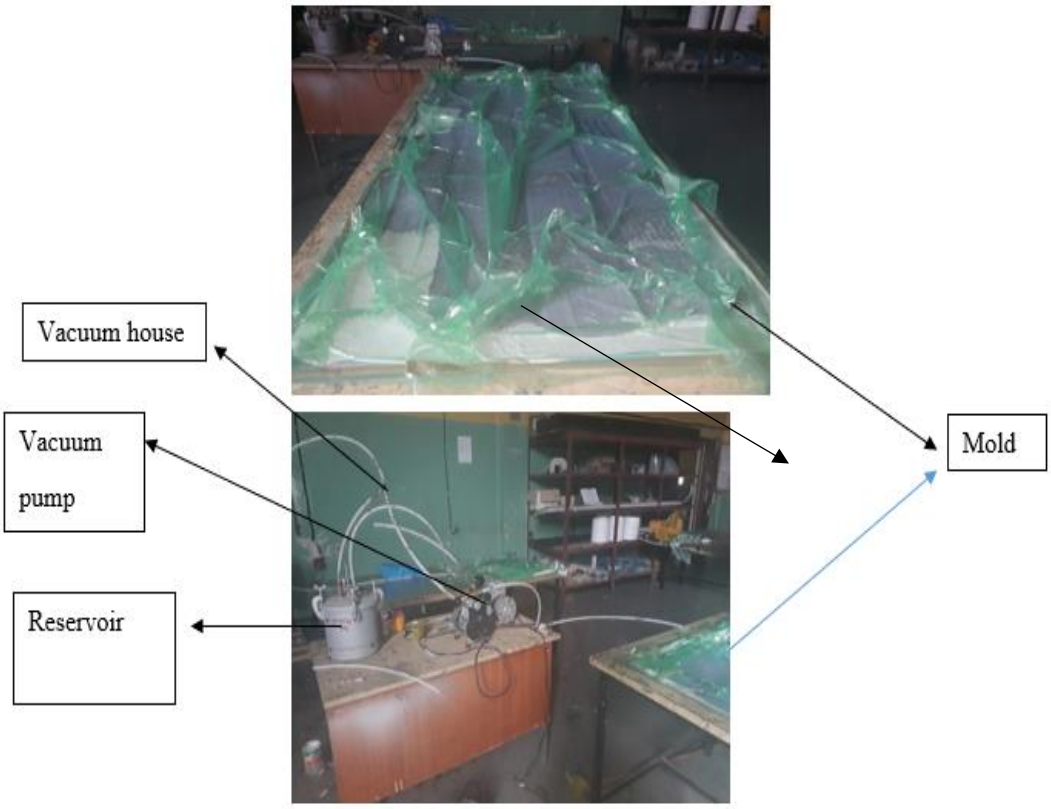

Figure 3-17 Composite manufacturing process

3.8.3.2. Dimension of specimen

From the prepared glass epoxy laminate, a specimen is cut for testing vibration properties. according to the ASTM E756 standard, the dimension of the specimen used for the vibration test was (180x30x3) millimeter. Different crack was introduced by using a hacksaw.

Figure 3-18 Specimens

3.8.3.3. Experimental setup

During the measurement of vibration LabVIEW software was used. The specimen was excited at certain points using a hammer. The accelerometer (ACC103) fitted with the specimen by a base wax. The LabVIEW software used to obtain the frequency spectrum after the analyzer receives the signal, which was captured by the accelerometer. Each sample fitted with the help of an iron clam as shown in the fig below. For all the sample a cantilever boundary condition was used. After the result get from the LabVIEW software amplitude verse frequency graphs were plotted using MATLAB. According to ASTM E756(Acoustics, 1998) standard dynamic properties of a composite structure measure as shown in Figure 3-18. National Instrument product NI USB-6009 data acquisition device integrated into the computer with LABVIEW (2017) software was used.

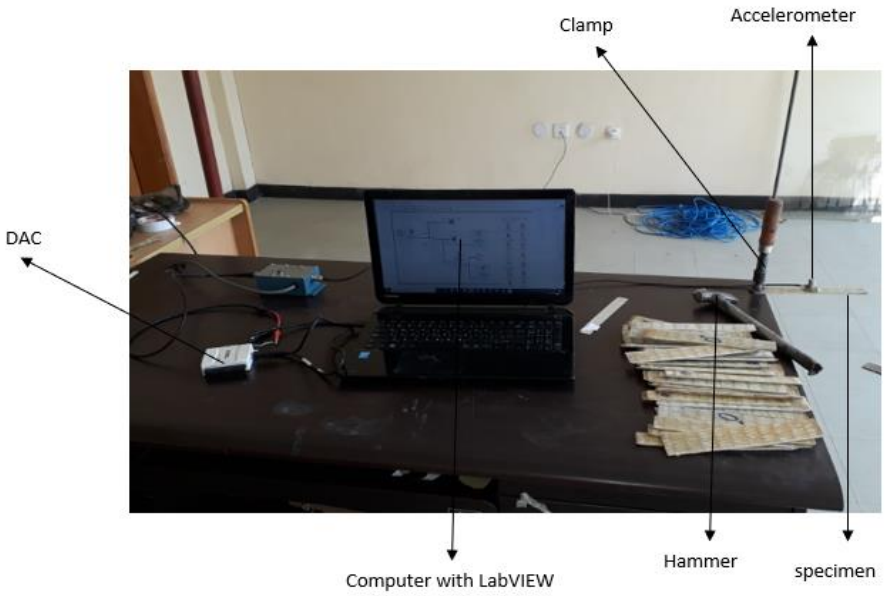

Figure 3-19 Experimental setup

LabVIEW software is used to record the data

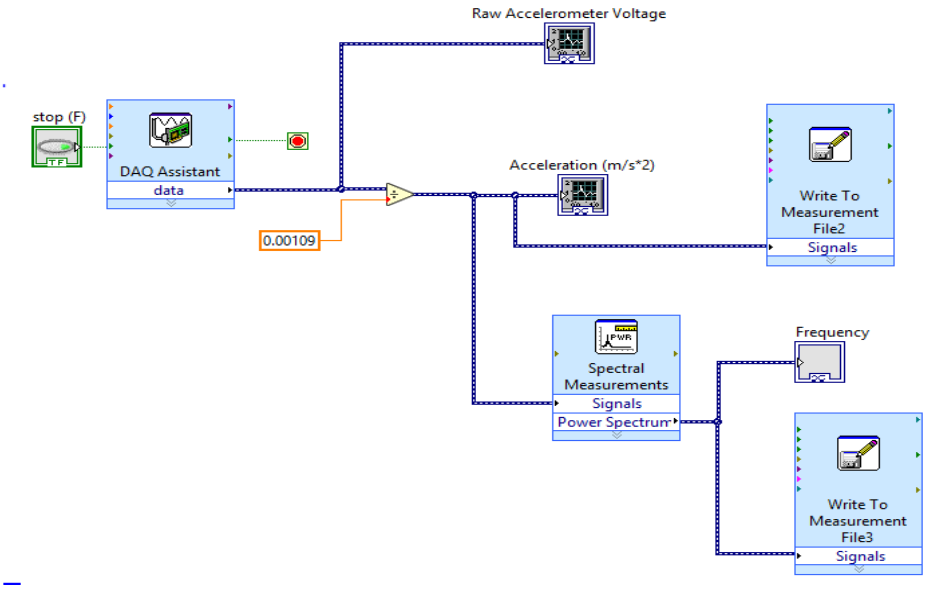

Figure 3-20 LABVIEW Block Diagram

Chapter Four

4. Result and Discussion

In this chapter, the result of the natural frequency for GFRP laminate using analytical, numerical and experimental methods was described and discussed. Using those methods, the analyses were conducted for both unidirectional and quasi-isotropic fiber arrangement. The analysis has been studied first for the laminate without a crack (uncracked) and second a laminate with crack (cracked) having different crack depth and crack location.

4.1. Analytical and numerical result of uncracked UD and QI GFRP cantilever beam

Free vibration analysis of a cantilever beam, to determine the natural frequency of unidirectional and quasi-isotropic composite laminate has been conducted analytical as equation 3.36 and numerical as described in section 3.9.2.1 for both unidirectional and quasi-isotropic laminate without crack. The natural frequency of the UD and QI laminate was determined by using Abaqus software. A typical spectrum diagram of the first, second and third natural frequencies of the unidirectional laminate was plotted in fig 4-1. The numerical and analytical results of the natural frequencies of the unidirectional E-glass fiber/epoxy composite beams without crack shown in Table 3

Table 3 Analytical and numerical result of natural frequencies of uncracked UD and QI laminate

Frequency (Hz)	laminate	Analytical	Numerical
First NF	UD	66.98	66.06
	QI	42.529	42.200
Second NF	UD	419.81	411.45
	QI	266.549	263.730
Third NF	UD	1175.30	1059.70
	QI	746.232	735.400

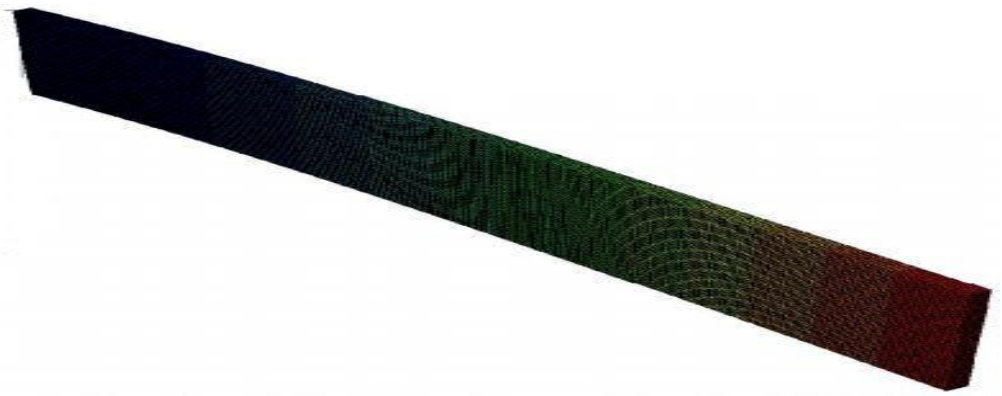

Step: Step- 1
Mode 1: Freq = 66.06 (cycle/time)

Step: Step- 1
Mode 2: Freq = 411.45 (cycle/time)

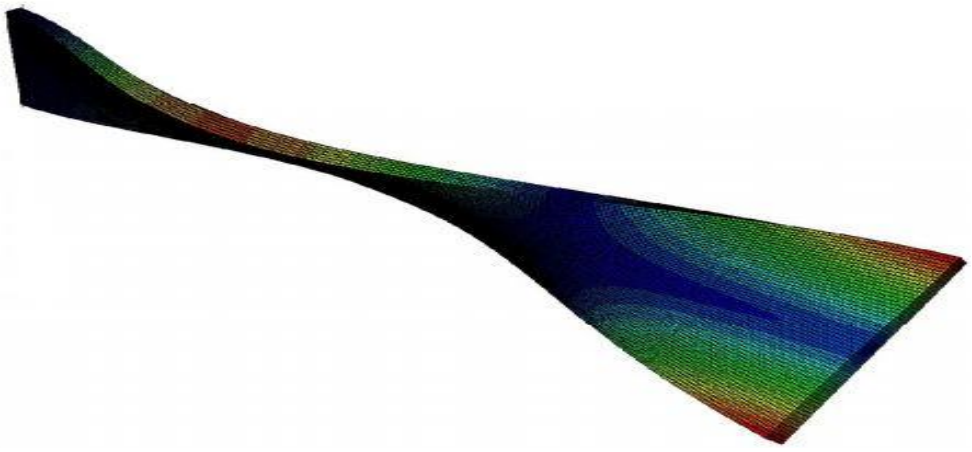

Step: Step- 1
Mode 3: Freq = 1059.70 (cycle/time)

Figure 4-1 The first three natural frequency for UD lamina orientation GFRP without crack

From table 3 the natural frequency for unidirectional laminate was higher than the natural frequency of quasi-isotropic laminate in all the three modes of vibration. This is due to the stiffness of the unidirectional laminate was higher than the quasi-isotropic laminate.

4.2. Analytical and numerical result of cracked UD and QI GFRP cantilever beam

The vibration properties of GFRP composite were affected by crack depth and crack location. First, for a crack location, one (45 mm from the fixed end) with different crack depth were analyzed, and second, the effect of crack location studied. To see the effect of crack depth on the vibration properties of GFRP material, a crack to width ratio from 0 to 0.5 will consider (Kim *et al.*, 2019). In this paper 3 mm, 5 mm, 10 mm, and 15 mm crack were introduced in the specimen and the first three natural frequencies were recorded.

4.2.1. Analytical result of UD and QI GFRP laminate for different crack depth

Using first-order shear deformation theory the natural frequencies of cracked unidirectional and quasi-isotropic composite laminate have been conducted using equation 3.38. As shown in Table 4, the crack depth affects the natural frequency in all three modes. For all three modes, the increase in crack depth decreases the natural frequency.

Table 4 Analytical result of natural frequencies for cracked UD and QI laminate

Frequency	laminate	Crack depth(mm)			
		3	5	10	15
First NF	UD	63.54	61.14	54.69	47.36
	QI	40.347	38.824	34.725	30.073
Second NF	UD	398.26	383.23	342.77	296.85
	QI	252.871	243.325	217.637	188.47
Third NF	UD	1114.98	1072.89	959.62	831.06
	QI	707.938	681.213	609.297	527.66

4.2.2. Numerical result of UD and QI GFRP laminate for different crack depth

Numerical analysis was performed for UD and QI laminate using Abaqus software, as the steps listed in section 3.9.2.1 and a local mesh was assigned for the cracked section. From the spectrum diagram, the value of the natural frequencies for the different modes was recorded. For each crack depth, a new model was developed and the result was recorded from the spectrum diagram. A typical natural frequency graph for 15mm crack depth unidirectional laminate was presented in fig 4-2. The result for the other crack depths was put in table 5.

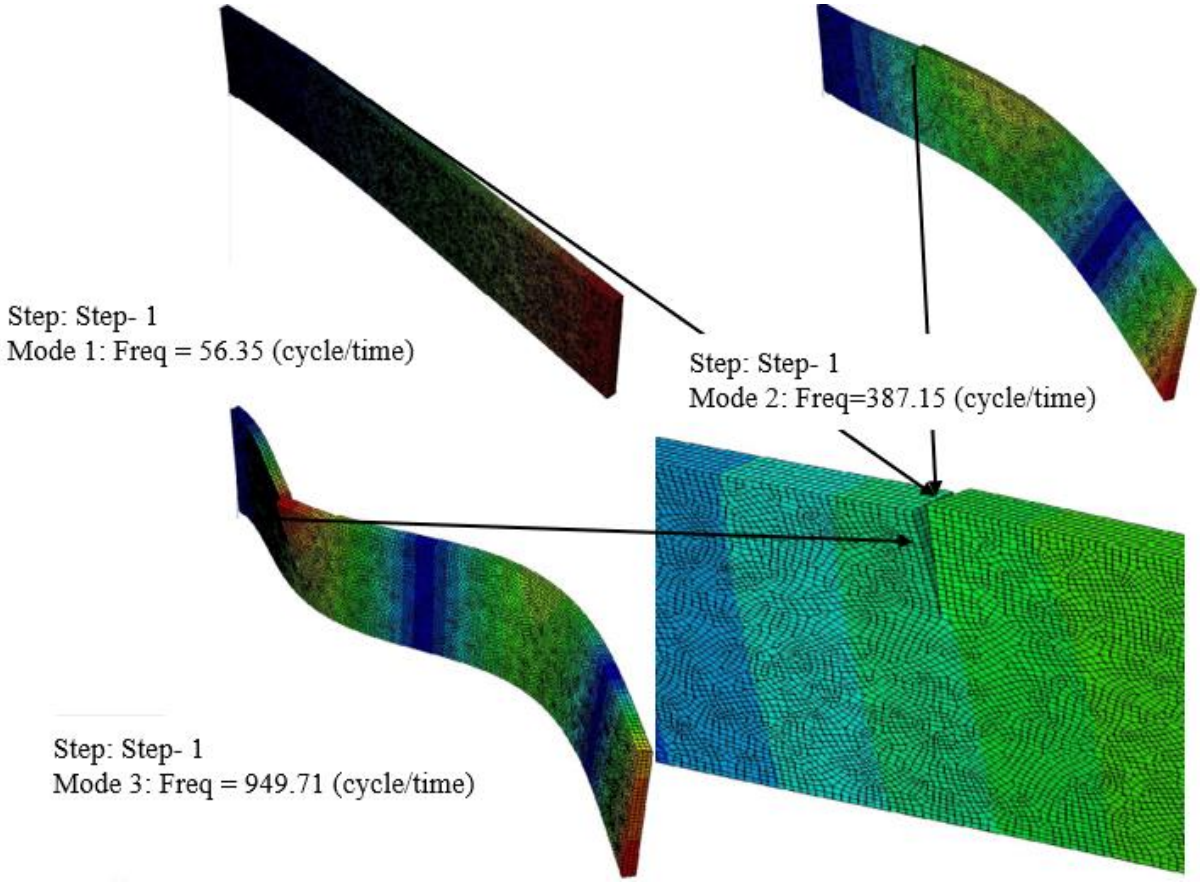

Figure 4-2 The first three natural frequency for UD laminate GFRP with 15mm crack

Table 5 Numerical result of natural frequencies for cracked UD and QI laminate

Frequency (Hz)	Laminate	Crack depth(mm)			
		3	5	10	15
First NF	UD	65.68	65.11	62.64	56.35
	QI	42.095	42.061	40.601	37.343
Second NF	UD	411.33	411.02	408.96	387.15
	QI	264.05	265.34	262.14	249.11
Third NF	UD	1058.60	1054.30	1030.90	949.71
	QI	734.13	734.47	713.15	664.06

As shown in Table 5, the natural frequency decrease as the crack depth increase for all the three modes of vibration. In both unidirectional and quasi-isotopic laminate, the natural frequency decrease but the decrease in natural frequency was different for the two-lamina orientation and this indicates that the change in natural frequency due to the crack depth also depends on the fiber arrangement. A typical crack depth verse first, second and third natural frequency graph described as follows.

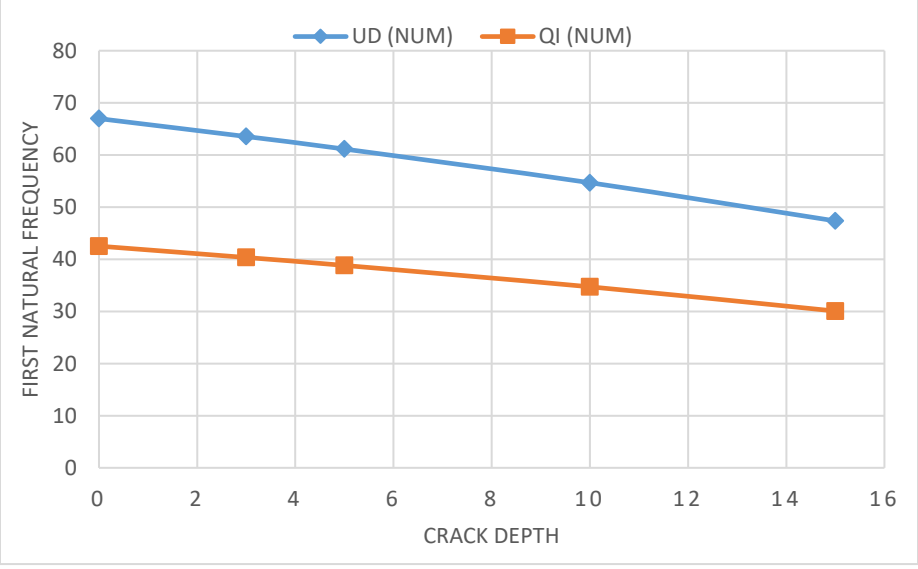

a

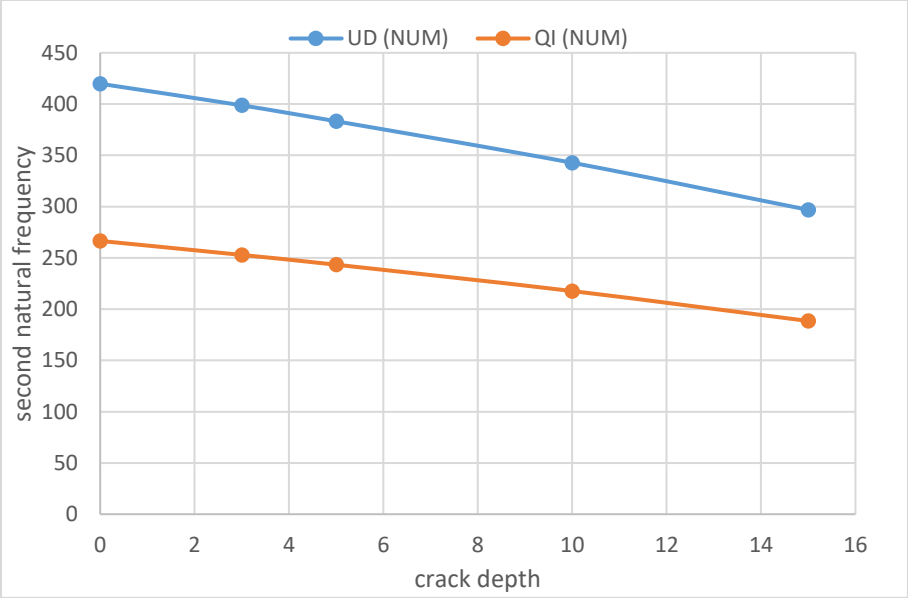

b

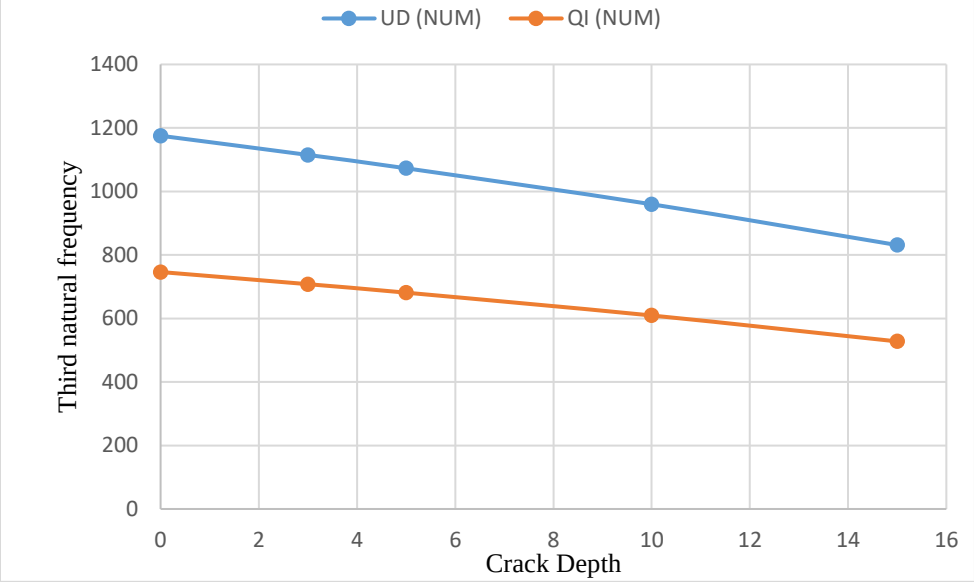

c

Figure 4-3 Natural frequency vs crack depth for UD and QI laminate a) First natural frequency b) Second natural frequency c) Third natural frequency

4.2.3. Numerical result of UD and QI GFRP laminate for different crack location

Using Abaqus software numerical analysis was performed for both unidirectional and quasi-isotropic laminate at different crack locations. To see the effect of crack location, on the vibration properties of GFRP material, three locations were selected. Which are, crack location one 45 mm, crack location two 90 mm and crack location three 135 mm from the fixed end. In this study, a constant crack depth (10 mm) was used for all three positions.

Table 6 Numerical result of natural frequencies for cracked UD and QI laminate with different crack location

Frequency	Laminate	Location one (45 mm)	Location two (90 mm)	Location three (135 mm)
First NF	UD	62.640	62.306	63.140
	QI	40.601	39.53	40.380
Second NF	UD	408.96	371.53	385.07
	QI	262.14	242.06	248.39
Third NF	UD	1030.90	997.49	985.15
	QI	713.15	707.70	674.24

The natural frequencies of the unidirectional laminate at the different crack locations were recorded from the spectrum diagram in the Abaqus software and to indicate the crack location, atypical ABAQUS graph for, the third mode of vibration was presented in fig 4-4, fig 4-5 and fig 4-6.

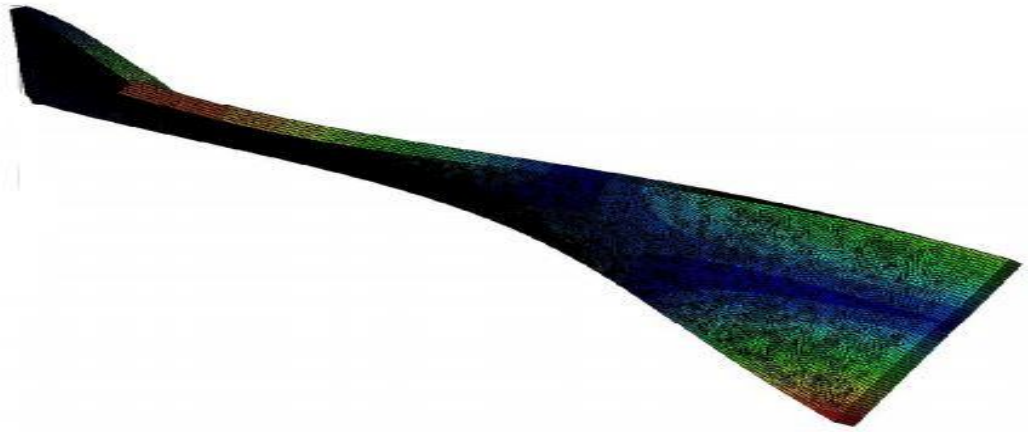

Step: Step- 1

Mode 3: Freq = 1030.90 (cycle/time)

Figure 4-4 Third natural frequency for UD laminate GFRP at crack location one

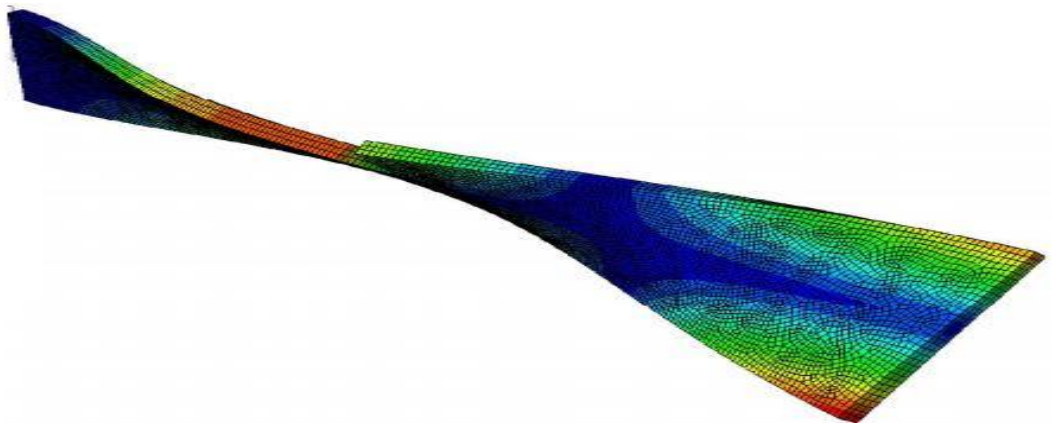

Step: Step- 1

Mode 3: Freq = 997.49 (cycle/time)

Figure 4-5 Third natural frequency for UD laminate GFRP at crack location two

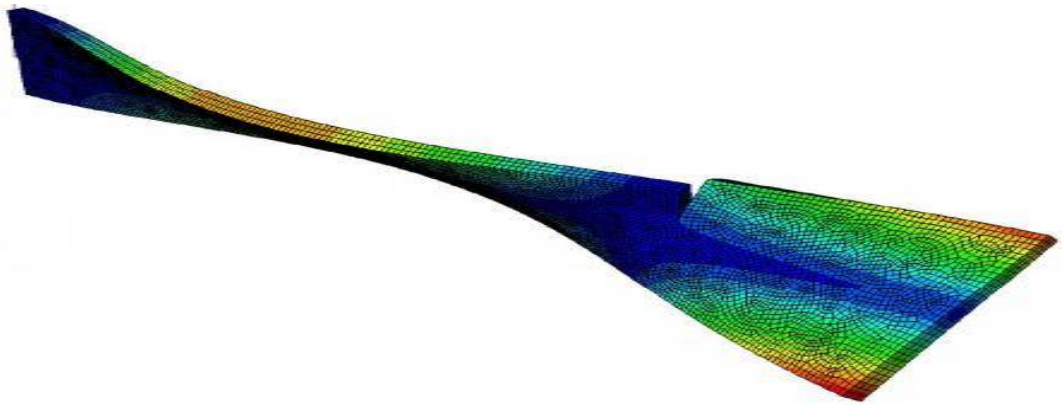

Step: Step- 1

Mode 3: Freq = 985.15 (cycle/time)

Figure 4-6 Third natural frequency for UD laminate GFRP at crack location three

The result indicates the natural frequencies vary with the change in the crack location. A typical natural frequency vs crack location graph for the first three modes of vibration was presented in fig 4-7 and fig 4-8 for unidirectional and quasi-isotropic laminate respectively.

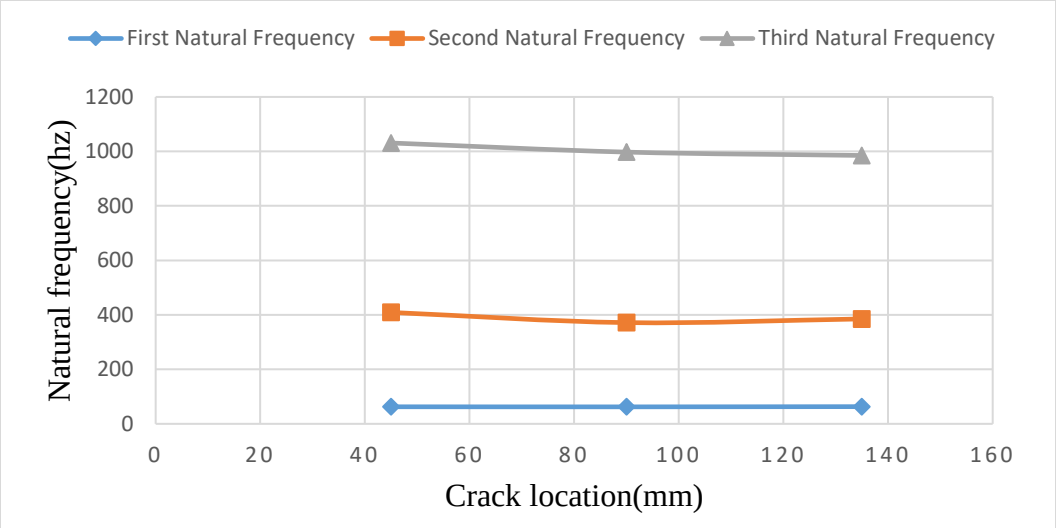

Figure 4-7 Natural frequency vs crack location for UD laminate

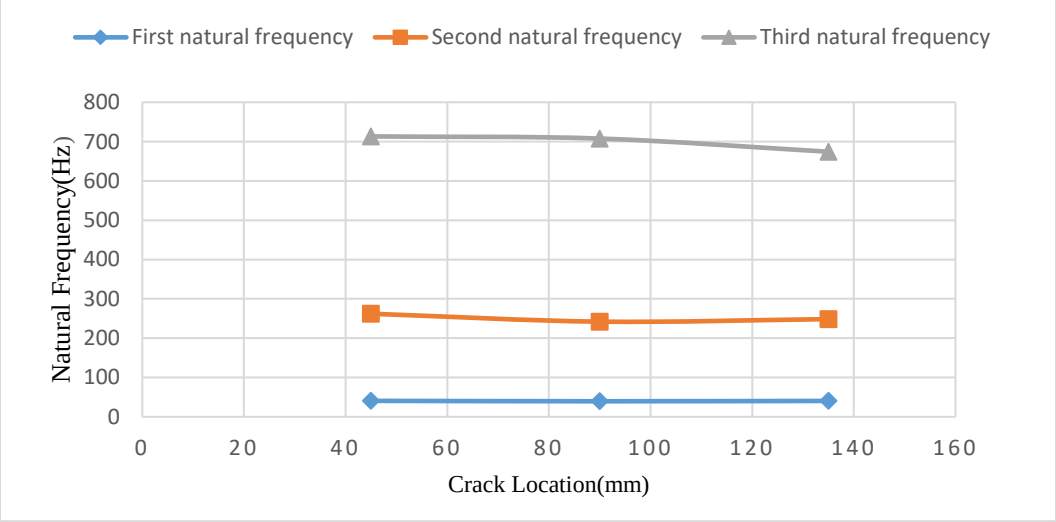

Figure 4-8 Natural frequency vs crack location for QI laminate

4.3. Experimental verification

4.3.1. Experimental result of uncracked UD and QI GFRP cantilever beam

GFRP were manufactured, with 50% fiber and 50% epoxy resin volume fraction, in [04]s and [0,90,45, -45] s lamina orientation. In this paper, for vibration analysis according to ASTM E756, a total of five specimens were used for repeatability and the mean value was taken. A free vibration test was done for unidirectional and quasi-isotropic laminate

without crack. As from the experimental set up the result recorded from the LabVIEW software was plotted as amplitude vs frequency graph or frequency response function graph using MATLAB software as shown in fig 4-9.

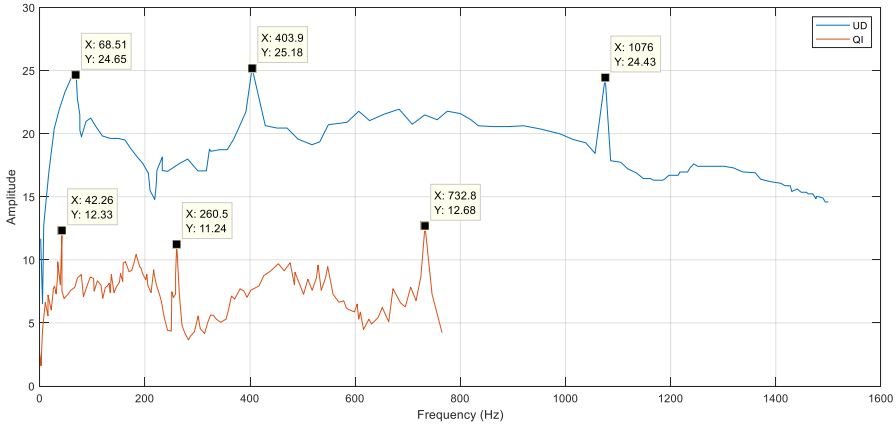

Figure 4-9 Frequency response function graph of uncracked UD and QI laminate

The value of the first, second and third natural frequencies taken from the graph and put in table 7.

Table 7 Experimental result of natural frequencies of uncracked UD and QI laminate

Frequency (Hz)	laminate	Experimental
First NF	UD	68.51
	QI	42.16
Second NF	UD	403.9
	QI	260.5
Third NF	UD	1176.0
	QI	732.8

4.3.2. Experimental result of UD and QI GFRP laminate for different crack depth

After the experimental test has been conducted for the GFRP without crack, different cracks introduced in the specimens, within 3mm, 5mm,10mm, and 15mm crack depth at constant crack location, which is 45 mm from the fixed end and a free vibration test was done for unidirectional and quasi-isotropic laminate. In the same way as the uncracked

beam the result for the first, second and third natural frequency taken from the frequency response function graph and put in table 8.

Table 8 Experimental result of natural frequencies of cracked UD and QI laminate

Frequency	laminate	Crack depth (mm)			
		3	5	5	15
First NF	UD	62.23	60.31	49.37	46.02
	QI	40.14	39.46	31.51	29.62
Second NF	UD	395.9	379.5	371.8	288.2
	QI	248.2	241.7	214.3	187.8
Third NF	UD	1111.0	1060.0	952.7	827.3
	QI	699.3	676.9	600.8	528.0

The first natural frequency decrease for both unidirectional and quasi-isotropic laminate for the crack depth, 3, 5, 10, and 15 mm considered at crack location one. Fig 4-10 shows the first natural frequency decrease as the crack depth increase and this graph shows the same decrement as the numerical result indicated by fig 4-3 a.

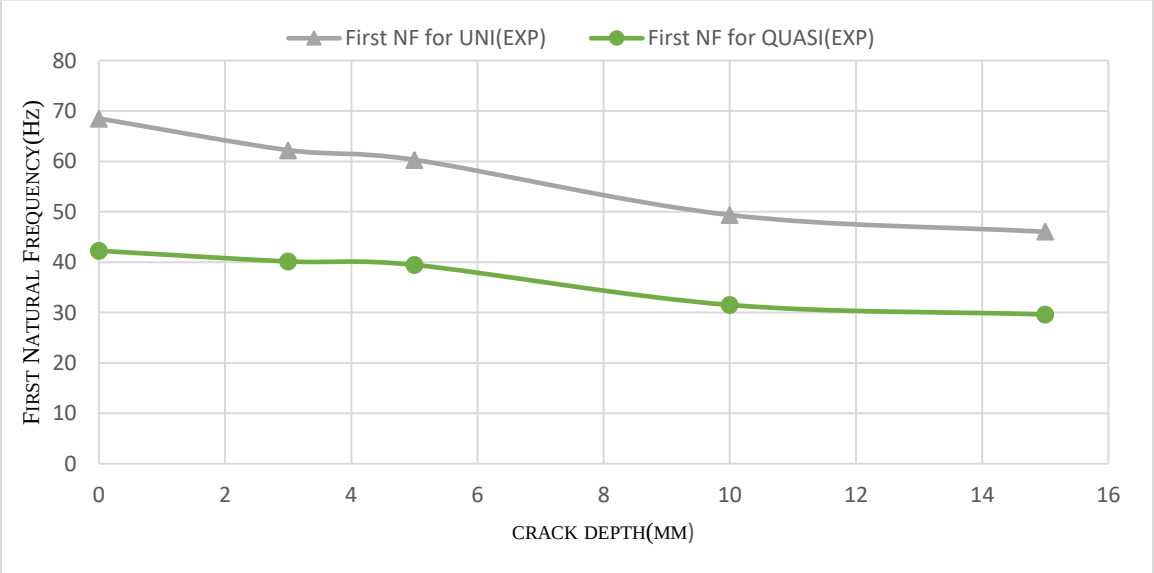

Figure 4-10 First Natural Frequency vs Crack Depth

It was observed that for the relative crack location of Lc/L= 0.25, the fundamental natural frequencies of unidirectional laminate reduced by 9.12%, 11.96%, 27.93%, and 32.82% for crack depths of 3, 5, 10, and 15 mm, respectively, as compared with the uncracked beam. Similarly, for the quasi-isotropic laminate, the fundamental natural frequency reduced by 1.89%, 5.01%, 25.43% and 29.91% for the crack depth 3, 5, 10 and 15 mm, respectively, as compared with the uncracked beam. As observed in both unidirectional and quasi-isotropic laminates, generally, the fundamental frequency decreased as the crack depth increased for a relative crack location Lc/L= 0.25. These findings are in good agreement with S.Vader et al (Vader *et al.*, 2017).

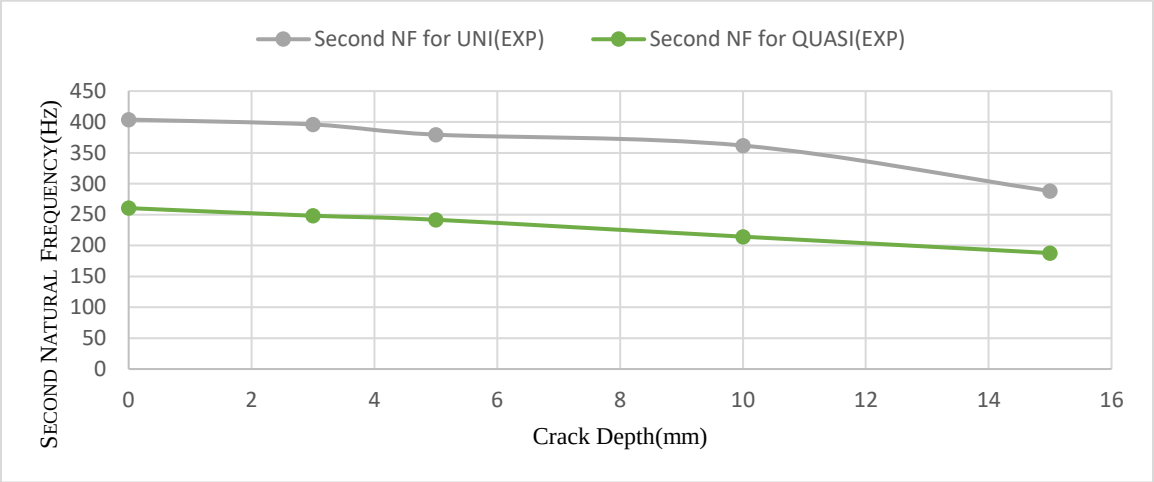

Figure 4-11 Second Natural Frequency vs Crack Depth

Figure 4-11 shows the second natural frequency of the unidirectional E glass fiber/epoxy composite the cantilever beam with different crack depth for both unidirectional and quasi-isotropic laminate. The frequency is higher than the fundamental frequency of the cracked composite beam. It is observed that the second natural frequency of unidirectional laminate for a relative crack location of Lc/L= 0.25 reduced by 2.02%, 6.04%, 7.94%, and 28.69% for crack depths of 3, 5, 10, and 15 mm, respectively, as compared with the corresponding uncracked beam. Similarly, for the quasi-isotropic laminate, the second natural frequency reduced by 4.72%, 7.21%, 17.31%, and 27.90 for crack depths of 3, 5, 10, and 15 mm, respectively, as compared with the corresponding uncracked beam.

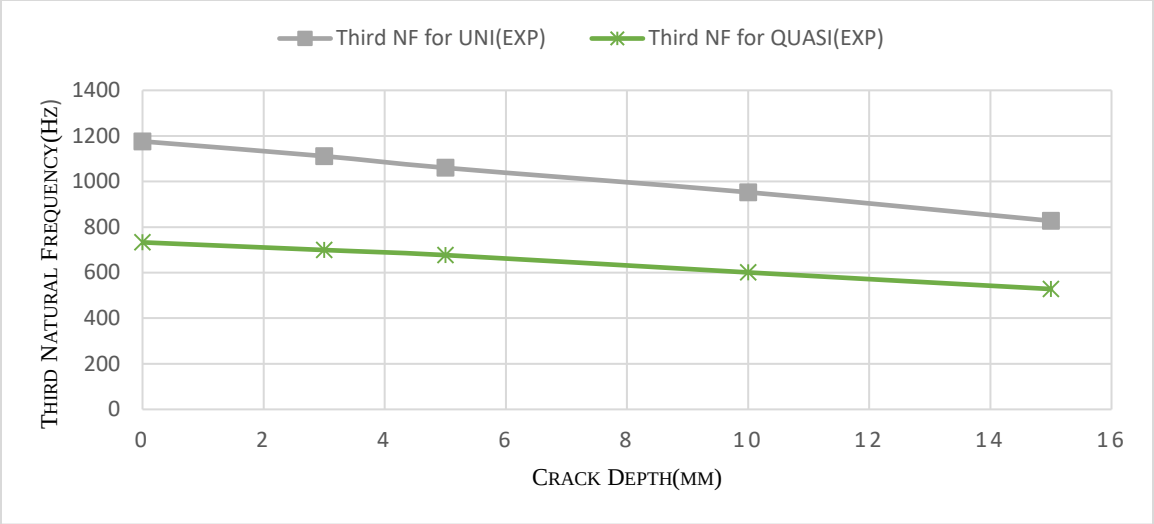

Figure 4-12 Third Natural Frequency vs Crack Depth

On the other hand, the introduction of cracks in both unidirectional and quasi-isotropic composite beams showed a slightly reduced effect on the third natural frequency, but the change in magnitude was less significant in the unidirectional composite beam. For the unidirectional laminate, the third natural frequency reduced by 0.5%, 1.48%, 11.45% and 23.11% for crack depths of 3, 5, 10, and 15 mm, respectively. Similarly, For the quasi-isotropic laminate, the third natural frequency reduced by 4.57%, 7.62%, 18.01 and 27.94% for the given crack depths of 3, 5, 10, and 15 mm, respectively. The graph from the experimental result in the first, second and third natural frequency graph shows the same decline as the numerical result plotted in fig 4-3.

4.3.3. Experimental result of UD and QI GFRP laminate for different crack location

For both unidirectional and quasi-isotropic laminate, the crack was introduced at a different location from the fixed end. The first crack location was 45 mm from the fixed end and the second and third crack locations were 90 mm and 135 mm from the fixed end at a constant crack depth of 10 mm respectively. the experimental test result with a different crack location for both UD and QI laminate as shown in table 9.

Table 9 Experimental result for both UD and QI GFRP at the different crack location

Frequency	Laminate	Crack location (mm)		
		45	90	135
First NF	UD	49.37	60.03	63.88
	QI	31.51	37.05	39.68
Second NF	UD	371.8	385.9	400.05
	QI	214.3	235.2	244.3
Third NF	UD	952.7	994.0	980.3
	QI	600.8	711.2	674.2

In both unidirectional and quasi-isotropic composite beams, the fundamental natural frequency decreased as the crack location moved from the fixed end to the middle of the beam. As the crack moved away from the mid-span to the free end, its effect is insignificant on the fundamental natural frequencies of the two materials configurations. This finding can be explained by the fact that the bending moment is maximum at a fixed end for a cantilever beam and gradually becomes zero at the free ends. Thus, the natural frequencies are almost unchanged when the crack is far away from the fixed end. This observation is in a perfect agreement with(Sahu and Das, 2020)(Agarwalla and Parhi, 2013).

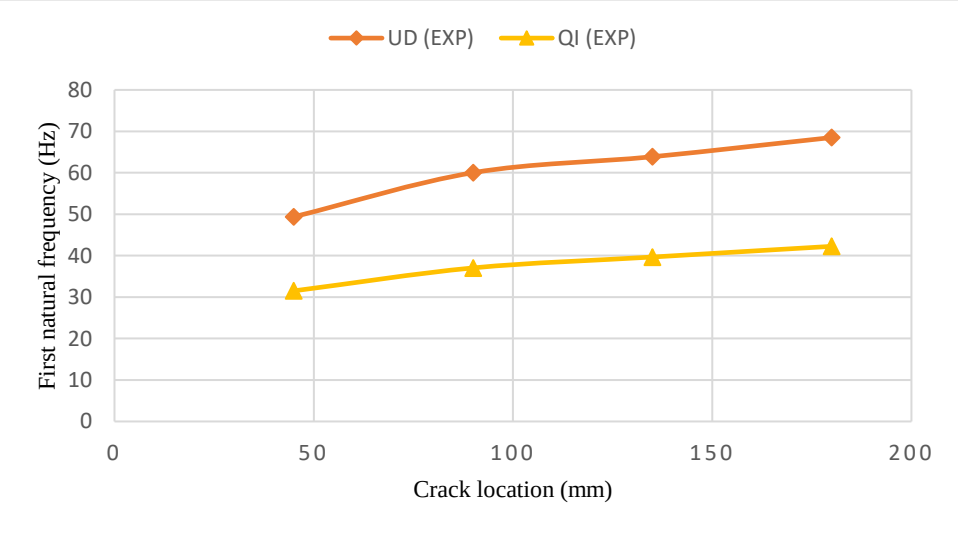

Figure 4-13Variation of the first natural frequencies at the various crack location for the UD and QI laminate of the cantilever beam, at constant crack depth

Figure 4-14 shows the variation of the second natural frequency of free vibration of the unidirectional and quasi-isotropic laminate beam with a relative crack location for constant crack depth. The second natural frequencies were higher than the fundamental natural frequencies for the cracked beam. The variation of the second natural frequencies due to the crack location shows a different variation with the fundamental natural frequencies. The second natural frequencies decreased around the mid-span of the beam due to the maximum curvature in the middle of the beam.

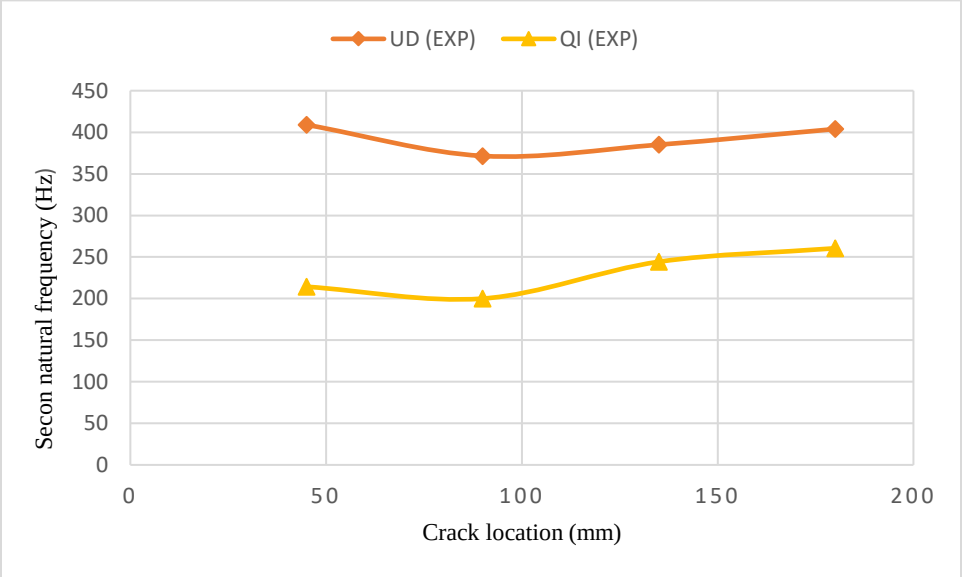

Figure 4-14 Variation of the second natural frequencies at the various crack location for the UD and QI laminate of the cantilever beam, at constant crack depth

Figure 4-15 shows the variation of the third natural frequency of free vibration of a unidirectional and quasi-isotropic laminate beam with a relative crack location for constant crack depth. The third natural frequencies were higher than the second natural frequencies for the cracked beam. The variation of the third natural frequencies due to the crack location shows a different variation with the fundamental and second natural frequencies. The third natural frequencies decreased from the fixed end to 0.25L of the beam and increase to the mid-span. The third natural frequency at the middle of the beam approaches to the uncracked beam and decreases to 0.75L and increases to the free end.

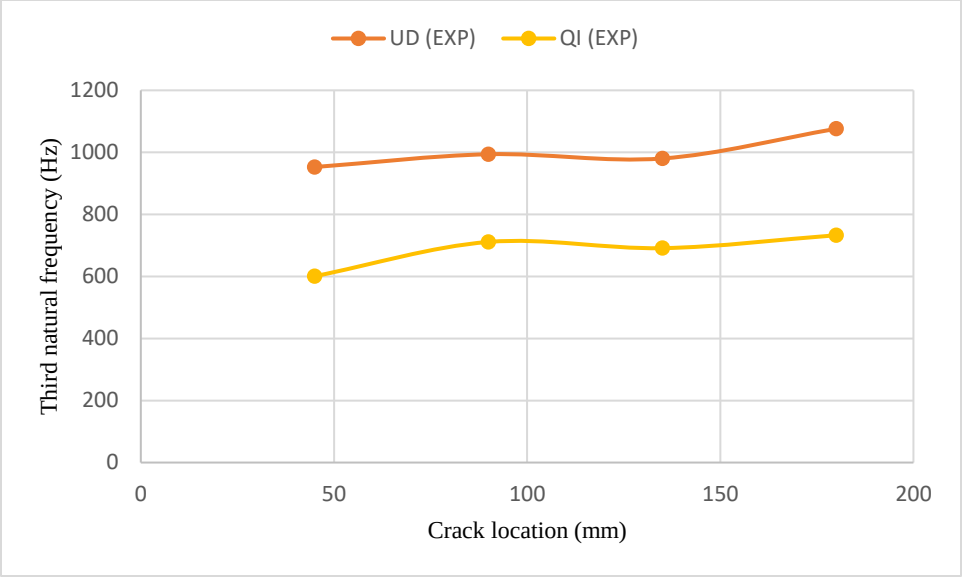

Figure 4-15 Variation of the third natural frequencies at the various crack location for the UD and QI laminate of the cantilever beam, at constant crack depth

The graph for the effect of crack location on the first, second and third natural frequency from the experimental result showed the same trend as the graph of numerical result, fig 4-7 and 4-8, and this indicates the numerical and experimental result shows good agreement. For different crack locations, the change in frequency for the different modes of vibration depends on the beam curvature. The location at which the curvature is high has a minimum natural frequency because stress depends on the geometry of the beam. At the point of curvature, the shape of the beam became circular and that increases the stress at that point. For example, the second mode of vibration the curvature is at the mid-span and that is the minimum natural frequency and for the third mode of vibration, there are two curvatures at 0.25L and 0.75L and that is the location the natural frequency was minimum. This is in perfect agreement with(Sahu and Das, 2020)(Banerjee, 2009)

As the results presented in the above section the location of the crack can be forecast. a crack near the fixed end decreases the first natural frequency and a crack at the middle of the beam decrease the second natural frequency while a crack around 0.25L and 0.75L decrease the third natural frequency. So, by using the first three natural frequencies we can predict the location of the crack. The depth of the crack can be estimated by the difference from the uncracked beam, the higher the difference in frequency between the cracked and the uncracked beam the deepest in the crack in all the three moods of vibration.

4.4. Comparison of results for different crack depth

In vibrational behaviors analysis of composite materials, three different methods were applied. Using the three methods, the results were described in the above result and discussion part and the comparisons are listed in this section.

Two error values were calculated. Which are error value one, the comparisons of the analytical result with the experimental result and error value two were the comparisons of numerical and experimental result. Errors were calculated for both unidirectional and quasi-isotropic laminate.

Table 10 Error values of the first, second and third natural frequencies of unidirectional laminate.

Crack depth(mm)	mode	Analytical	Numerical	Experimental	Error 1 %	Error 2 %
0	1	66.98	66.06	68.51	2.23	3.57
	2	419.81	411.45	403.9	3.93	1.86
	3	1175.3	1059.7	1176	9.88	0.59
3	1	63.54	65.687	62.23	2.10	5.55
	2	398.266	411.33	395.9	0.59	3.89
	3	1114.99	1058.6	1111	0.35	4.71
5	1	61.14	65.114	60.31	1.37	7.96
	2	383.233	411.02	379.5	0.98	8.30
	3	1072.9	1054.3	1060	1.21	0.53
10	1	54.69	62.640	49.37	10.77	21.11
	2	342.774	408.96	371.8	7.80	9.99
	3	959.628	1030.9	952.7	0.72	7.58
15	1	47.36	56.350	46.02	2.911	18.33
	2	296.851	387.15	288.2	3.00	25.55
	3	831.063	949.71	827.3	0.45	12.89

Table 11 Error values of the first, second and third natural frequencies of Quasi isotopic laminate.

Crack depth(mm)	mode	Analytical	Numerical	Experimental	Error 1 %	Error 2 %
0	1	42.529	42.200	42.26	0.61	0.14
	2	266.549	263.73	260.5	2.32	1.23
	3	746.23	735.4	732.8	1.83	0.35
3	1	40.34	42.09	39.46	2.23	6.66
	2	252.87	264.05	248.2	1.88	6.38
	3	707.93	734.13	699.3	1.23	4.98
5	1	38.82	42.06	40.14	3.28	4.78
	2	243.32	265.34	241.7	0.67	9.78
	3	681.21	734.47	676.9	0.63	8.50
10	1	34.72	40.06	31.51	10.18	20.13
	2	217.63	262.14	214.3	1.55	18.25
	3	609.29	713.15	600.8	1.41	15.75
15	1	30.07	37.04	29.62	1.51	20.03
	2	188.47	249.11	187.8	0.35	24.61
	3	527.66	664.06	528	0.06	20.49

Form table 10 and table 11 the difference between the numerical and the experimental results were due to the experimental analyses considers all the manufacturing fault, defects and also environmental effect during the test. Due to this the experimental analysis was smaller than the numerical results. The error will higher when the crack depth increases because the stress was intensified for high crack depth during the introduction of crack.

4.5. Comparison of result for different fiber orientation

The fundamental frequency for quasi-isotropic laminate is lower than the unidirectional laminate. because of the increase in fiber orientation decrease, the stiffens of the cracked composite laminate. For the same crack depths and location, the change in the fundamental natural frequency of the unidirectional laminate was higher than that of the quasi-isotropic laminate as compared with the respective uncracked beam. These findings implied that the

detrimental effect of the presence of a crack in the composite beam depends on fiber orientation and crack geometries.

Table 12 Experimental result for both unidirectional and quasi-isotropic laminate GFRP

Frequency	laminate	Crack depth (mm)				
		0	3	5	10	15
First NF	UD	68.51	62.23	60.31	49.37	46.02
	QI	42.26	39.46	40.14	31.51	29.62
Second NF	UD	403.9	395.9	379.5	371.8	288.2
	QI	260.5	248.2	241.7	214.3	187.8
Third NF	UD	1076.0	1111.0	1060.0	952.7	827.3
	QI	732.8	699.3	676.9	600.8	528.0

Generally as shown in table 12 the natural frequency of GFRP composite material depends on the fiber arrangement since the natural frequency was different for UD and QI laminate and the effect of crack also depends on the fiber arrangement, as the crack depth increase the natural frequencies in all the three modes decrease but the decrease in the UD and QI laminate were different.

Chapter Five

5. Conclusion and Recommendations

5.1. Conclusion

Considering the increasing use of fiber-reinforced polymer in many engineering applications because of their high strength to weight ratio. This study was conducted to analyze the effect of crack on vibration properties especially the natural frequency of UD and QI laminate with different crack depth and crack locations.

In this study, FSDT was used to study the natural frequency of asymmetrical laminated composite cantilever beam with an open edge crack. The analytical, numerical and experimental studies were conducted for the free vibration analysis of unidirectional fiberglass/epoxy laminate.

From the present study, the following conclusions are drawn.

- The natural frequencies were higher for unidirectional laminate than quasi-isotropic laminate.
- The introduction of crack decreases the natural frequency of a composite laminate.
- For both unidirectional and quasi-isotropic laminate, the increase in crack depth decreases the natural frequencies in all the three modes of vibration for a constant crack location.
- the natural frequency of the cracked unidirectional and quasi-isotropic laminate was affected by the location of the crack.
- the change of the natural frequency was different for the first, second and third modes of vibration.
- Using unidirectional fiber with different lamina orientation it is possible to create a structure with different vibration properties.
- In all the three methods the effect of crack depth on natural frequency and the change in natural frequency with crack location shows the same trend.

From the result, it was concluded that crack of different depth at a different crack location for different lamina orientation affects the vibration properties of a composite laminate.

The result shows that crack introduces in composite material changes the vibration properties of the material and crack on a specimen decrease the natural frequency in the

first three modes of vibration for different lamina orientation. This study can be used to monitor the structure element by considering the change in the vibration of composite laminate due to different crack.

5.2. Recommendations

The recommendation from this paper is that using ABAQUS CAE software is good to predict the vibration properties of GFRP composite material. From the results, it has been seen the stiffens of the material are changed due to edge crack, and that affects the natural frequency of the GFRP composite material. But edge crack is not the only cause that affects the vibration properties of GFRP composite. So, manufacturers must consider other parameters like delamination for the change in the material stiffens. As shown from the research, the natural frequency is higher for unidirectional lamina orientation than quasi-isotropic lamina orientation. So, it is recommended that for manufacturers by changing the lamina orientation it is possible to get the different working frequencies.

5.3. Future work

This paper mainly addresses the effect of crack location and crack depth on natural frequency for a cantilever beam with unidirectional and quasi-isotropic lamina orientation. But there is some related research area studied in the future which are;

- The effect of different support types on the natural frequency of GFRP composite.
- The effect of volume fraction on natural frequency and damping properties

Reference

Acoustics, E. (1998) ‘Standard Test Method for Measuring Vibration-Damping Properties of Materials 1’.

Agarwalla, D. K. and Parhi, D. R. (2013) ‘Effect of Crack on Modal Parameters of a Cantilever Beam Subjected to Vibration’. Elsevier B.V., 51(NUiCONE 2012), pp. 665–669. doi: 10.1016/j.proeng.2013.01.094.

Aspragathos, N. A. (2016) ‘Identification of Crack Location and Magnitude in a Cantilever Beam From the Vibration Modes’, (May 1990). doi: 10.1016/0022-460X(90)90593-O.

Banerjee, J. R. (2009) ‘On the dynamic of cracked beam’, (May), pp. 1–11.

Barad, K. H., Sharma, D. S. and Vyas, V. (2013) ‘Crack detection in cantilever beam by frequency based method’, *Procedia Engineering*. Elsevier B.V., 51(NUiCONE 2012), pp. 770–775. doi: 10.1016/j.proeng.2013.01.110.

Belarbi, M. O. *et al.* (2017) ‘On the free vibration analysis of laminated composite and sandwich plates: A layerwise finite element formulation’, *Latin American Journal of Solids and Structures*, 14(12), pp. 2265–2290. doi: 10.1590/1679-78253222.

Borgaonkar, A. V, Mandale, M. B. and Potdar, S. B. (2018) ‘ScienceDirect Effect of Changes in Fiber Orientations on Modal Density of Fiberglass Composite Plates’, *Materials Today: Proceedings*. Elsevier Ltd, 5(2), pp. 5783–5791. doi: 10.1016/j.matpr.2017.12.175.

Chavan, S. S. and Joshi, M. M. (2015) ‘STUDY ON VIBRATION ANALYSIS OF COMPOSITE PLATE’, (4), pp. 69–76.

Das, M. T. (2018) ‘Experimental modal analysis of curved composite beam with transverse open crack’, 436, pp. 155–164. doi: 10.1016/j.jsv.2018.09.021.

Degefe, S. Y. (2015) ‘Finite Element Analysis of E-glass / Epoxy Composite for Automotive Structures’, pp. 1–81.

Edition, T. (no date) ‘PRINCIPLES OF COMPOSITE MATERIAL’.

Flight, S. (2019) ‘NASA Reference Publication 1351 Basic Mechanics of Laminated Composite Plates’, (October 1994).

Ghoneam, S. M. (1995) ‘Dynamic analysis of open cracked laminated composite beams’, 32, pp. 3–11.

Gowda, K. (2018) ‘“ VIBRATION ANALYSIS OF CANTILEVER BEAM OF

DIFFERENT MATERIALS ” Submitted In partial fulfillment of requirements for the award of in Submitted by’, (August).

‘Guide to Composites’ (2012). Available at: http://www.netcomposites.com/education.asp?sequence=2.

Heydari, M., Ebrahimi, A. and Behzad, M. (2014) ‘Engineering Science and Technology , an International Journal Forced vibration analysis of a Timoshenko cracked beam using a continuous model for the crack’, *Engineering Science and Technology, an International Journal*. Elsevier Ltd, 17(4), pp. 194–204. doi: 10.1016/j.jestch.2014.05.003.

Jassim, Z. A. *et al.* (2013) ‘A review on the vibration analysis for a damage occurrence of a cantilever beam’, *Engineering Failure Analysis*. Elsevier Ltd, 31, pp. 442–461. doi: 10.1016/j.engfailanal.2013.02.016.

Kahya, V. *et al.* (2019) ‘International Journal of Mechanical Sciences Free vibrations of laminated composite beams with multiple edge cracks : Numerical model and experimental validation’, 159(May), pp. 30–42. doi: 10.1016/j.ijmecsci.2019.05.032.

Kim, K. *et al.* (2019) ‘A modeling method for vibration analysis of cracked laminated composite beam of uniform rectangular cross-section with arbitrary boundary condition’, *Composite Structures*. Elsevier, 208(October 2018), pp. 127–140. doi: 10.1016/j.compstruct.2018.10.006.

Krawczuk, M., Ostachowicz, W. and Zak, A. (1997) ‘Modal analysis of cracked, unidirectional composite beam’, 1694(97), pp. 641–650.

Mr. Vishal S. Jagadale, P. L. B. R. and PG (2016) ‘EXPERIMENTAL INVESTIGATION of MECHANICAL PROPERTIES of GLASS FIBER / EPOXY COMPOSITES WITH’, 3(1), pp. 188–192. doi: 10.17148/IARJSET/ICAME.36.

Of, D. *et al.* (2018) ‘Design and development of hybrid composite mono leaf spring for light vehicle application’.

P.K. Mallik (2007) *FIBER- REINFORCED*. THIRD EDIT.

Patil, R. R., Verma, P. D. and Student, P. G. (2016) ‘Free Vibrational Analysis of Cracked and Un-cracked Cantilever Beam’, pp. 260–277.

Rao, S. S. (no date) *Fifth Edition*.

Ratnaparkhi, S. U. and Sarnobat, S. S. (2013) ‘Vibration Analysis of Composite Plate’, 3(1), pp. 377–380.

Raton, B. (1995) *practical analysis of composite laminates*.

Reddy, J. N. (1997) 'On locking-free shear deformable beam finite elements', *Computer Methods in Applied Mechanics and Engineering*, 149(1–4), pp. 113–132. doi: 10.1016/S0045-7825(97)00075-3.

Richardson, D. (no date) 'The Fundamental Principles of Composite Material Stiffness Predictions'.

Sahu, S. K. and Das, P. (2020) 'Experimental and numerical studies on vibration of laminated composite beam with transverse multiple cracks', *Mechanical Systems and Signal Processing*. Elsevier LTD, 135, p. 106398. doi: 10.1016/j.ymssp.2019.106398.

Shaat, M. *et al.* (2016) 'International Journal of Mechanical Sciences Modeling and Vibration Characteristics of Cracked Nano-Beams Made of Nanocrystalline Materials', 116, pp. 574–585. doi: 10.1016/j.ijmecsci.2016.07.037.

Sudheer, M., Pradyoth, K. R. and Somayaji, S. (2015) 'Analytical and Numerical Validation of Epoxy / Glass Structural Composites for Elastic Models', 5, pp. 162–168. doi: 10.5923/c.materials.201502.32.

Swamy, B. N., Lakshmaiah, C. and Reddy, K. T. (2017) 'Modeling and Analysis of Light Vehicle Chassis Made of Composite Material', 7(3), pp. 5011–5015.

Vader, S. S. *et al.* (2017) 'Crack detection in composite cantilever beam by Vibration analysis and Numerical method', pp. 1776–1785.

Yogesha, B. (2017) 'ScienceDirect Studies on Natural / Glass Fiber Reinforced Polymer Hybrid Composites : An Evolution', *Materials Today: Proceedings*. Elsevier Ltd, 4(2), pp. 2739–2747. doi: 10.1016/j.matpr.2017.02.151.

Appendix

1. Frequency response function graph

The frequency response graph for unidirectional laminate with different crack depth

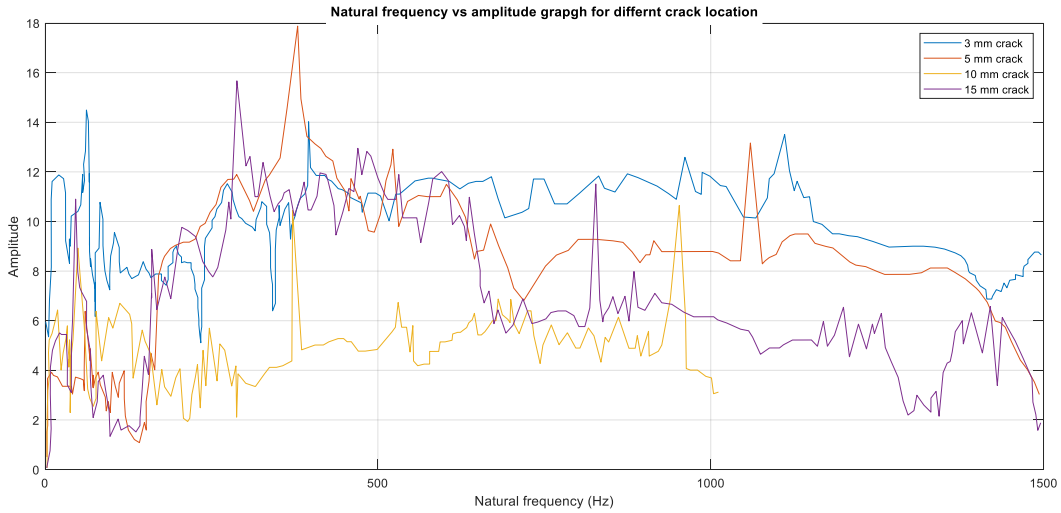

Frequency response graph for quasi-isotropic laminate with different crack location

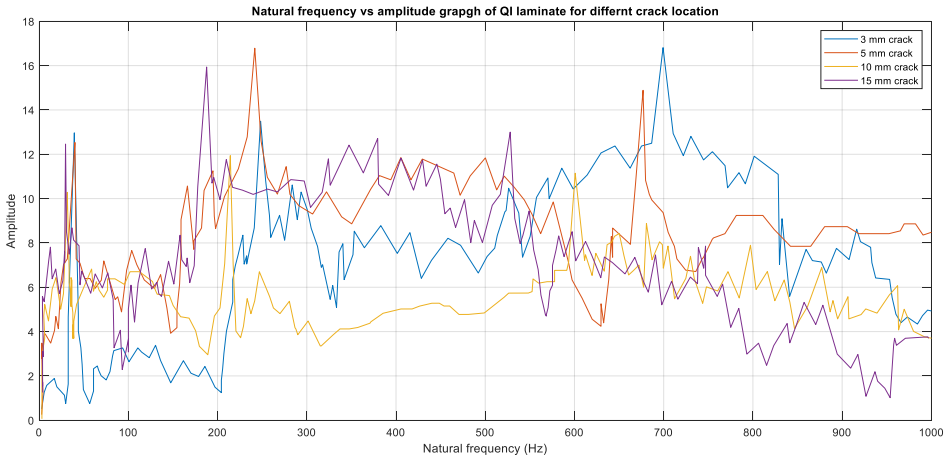

From the graph the first, second and third natural frequency were recorded and put in table. As in the experimental setup five specimen were used and from the result the mean value was taken. For instance, for a unidirectional beam with 3 mm crack depth the value for the first natural frequencies were 62.11, 62.20, 62.13, 62.35 and 62.39 and the mean value was 62.23 which put in table 8. In the same way the mean values were calculated for each sample and put in table.

2. Force and displacement relation ship

Based on first order shear deformation theory the constitutive equation of laminated plate can be expressed as follow

$$\begin{bmatrix} Nx \\ Ny \\ Nxy \\ Mx \\ My \\ Mxy \end{bmatrix} = \begin{bmatrix} \boldsymbol{A11} & A12 & A16 & \boldsymbol{B11} & B12 & B16 \\ A12 & A22 & A26 & B12 & B22 & B26 \\ A16 & A26 & A66 & B16 & B26 & B66 \\ \boldsymbol{B11} & B12 & B16 & \boldsymbol{D11} & D12 & D16 \\ B12 & B22 & B26 & D12 & D22 & D26 \\ B16 & B26 & B66 & D16 & D26 & D66 \end{bmatrix} = \begin{bmatrix} \varepsilon xx^0 \\ \varepsilon xy^0 \\ \varepsilon yy^0 \\ kxx^0 \\ kxy^0 \\ kyy^0 \end{bmatrix}$$

$$\begin{bmatrix} Qx \\ Qy \end{bmatrix} = \begin{bmatrix} A44 & A45 \\ A45 & A55 \end{bmatrix} = \begin{Bmatrix} \gamma xz^0 \\ \gamma yz^0 \end{Bmatrix}$$

3. Abaqus coding

```
# -*- coding: mbcs -*-
# Do not delete the following import lines
from abaqus import *
from abaqusConstants import *
import __main__

def Macro1():
    import section
    import regionToolset
    import displayGroupMdbToolset as dgm
    import part
    import material
    import assembly
    import step
    import interaction
    import load
    import mesh
    import optimization
    import job
    import sketch
    import visualization
    import xyPlot
    import displayGroupOdbToolset as dgo
    import connectorBehavior
    s = mdb.models['Model-1'].ConstrainedSketch(name='__profile__', sheetSize=0.2)
    g, v, d, c = s.geometry, s.vertices, s.dimensions, s.constraints
    s.sketchOptions.setValues(decimalPlaces=3)
    s.setPrimaryObject(option=STANDALONE)
    session.viewports['Viewport: 1'].view.setValues(nearPlane=0.158972,
        farPlane=0.218152, width=0.213805, height=0.0908333)
```

```
s.rectangle(point1=(0.095, 0.01), point2=(-0.09, -0.015))
s.ObliqueDimension(vertex1=v[1], vertex2=v[2], textPoint=(-0.0757144317030907,
    -0.0234655104577541), value=0.18)
s.ObliqueDimension(vertex1=v[2], vertex2=v[3], textPoint=(-0.0951334163546562,
    -0.00363273918628693), value=0.03)
p = mdb.models['Model-1'].Part(name='Part-1', dimensionality=THREE_D,
    type=DEFORMABLE_BODY)
p = mdb.models['Model-1'].parts['Part-1']
p.BaseSolidExtrude(sketch=s, depth=0.003)
s.unsetPrimaryObject()
p = mdb.models['Model-1'].parts['Part-1']
session.viewports['Viewport: 1'].setValues(displayedObject=p)
del mdb.models['Model-1'].sketches['__profile__']
session.viewports['Viewport: 1'].partDisplay.setValues(sectionAssignments=ON,
    engineeringFeatures=ON)
session.viewports['Viewport: 1'].partDisplay.geometryOptions.setValues(
    referenceRepresentation=OFF)
mdb.models['Model-1'].Material(name='Material-1')
mdb.models['Model-1'].materials['Material-1'].Density(table=((1910.0, ), ))
mdb.models['Model-1'].materials['Material-1'].Elastic(
    type=ENGINEERING_CONSTANTS, table=((38275000000.0, 6589000000.0,
    6589000000.0, 0.285, 0.05, 0.05, 2450000000.0, 2450000000.0,
    3140000000.0), ))
p = mdb.models['Model-1'].parts['Part-1']
v1 = p.vertices
p.DatumCsysByThreePoints(origin=v1[4], name='Datum csys-1',
    coordSysType=CARTESIAN, line1=(1.0, 0.0, 0.0), line2=(0.0, 1.0, 0.0))
layupOrientation = mdb.models['Model-1'].parts['Part-1'].datums[2]
p = mdb.models['Model-1'].parts['Part-1']
c = p.cells
cells = c.getSequenceFromMask(mask=('[#1 ]', ), )
region1=regionToolset.Region(cells=cells)
p = mdb.models['Model-1'].parts['Part-1']
c = p.cells
cells = c.getSequenceFromMask(mask=('[#1 ]', ), )
region2=regionToolset.Region(cells=cells)
p = mdb.models['Model-1'].parts['Part-1']
c = p.cells
cells = c.getSequenceFromMask(mask=('[#1 ]', ), )
region3=regionToolset.Region(cells=cells)
p = mdb.models['Model-1'].parts['Part-1']
c = p.cells
cells = c.getSequenceFromMask(mask=('[#1 ]', ), )
region4=regionToolset.Region(cells=cells)
compositeLayup = mdb.models['Model-1'].parts['Part-1'].CompositeLayup(
    name='CompositeLayup-1', description='', elementType=SOLID,
```

```
    symmetric=True, thicknessAssignment=FROM_SECTION)
compositeLayup.ReferenceOrientation(orientationType=SYSTEM,
    localCsys=layupOrientation, fieldName='',
    additionalRotationType=ROTATION_NONE, angle=0.0,
    additionalRotationField='', axis=AXIS_1, stackDirection=STACK_1)
compositeLayup.CompositePly(suppressed=False, plyName='Ply-1', region=region1,
    material='Material-1', thicknessType=SPECIFY_THICKNESS,
    thickness=0.000375, orientationType=SPECIFY_ORIENT,
    orientationValue=0.0, additionalRotationType=ROTATION_NONE,
    additionalRotationField='', axis=AXIS_3, angle=0.0, numIntPoints=1)
compositeLayup.CompositePly(suppressed=False, plyName='Ply-2', region=region2,
    material='Material-1', thicknessType=SPECIFY_THICKNESS,
    thickness=0.000375, orientationType=SPECIFY_ORIENT,
    orientationValue=0.0, additionalRotationType=ROTATION_NONE,
    additionalRotationField='', axis=AXIS_3, angle=0.0, numIntPoints=1)
compositeLayup.CompositePly(suppressed=False, plyName='Ply-3', region=region3,
    material='Material-1', thicknessType=SPECIFY_THICKNESS,
    thickness=0.000375, orientationType=SPECIFY_ORIENT,
    orientationValue=0.0, additionalRotationType=ROTATION_NONE,
    additionalRotationField='', axis=AXIS_3, angle=0.0, numIntPoints=1)
compositeLayup.CompositePly(suppressed=False, plyName='Ply-4', region=region4,
    material='Material-1', thicknessType=SPECIFY_THICKNESS,
    thickness=0.000375, orientationType=SPECIFY_ORIENT,
    orientationValue=0.0, additionalRotationType=ROTATION_NONE,
    additionalRotationField='', axis=AXIS_3, angle=0.0, numIntPoints=1)
p = mdb.models['Model-1'].parts['Part-1']
session.viewports['Viewport: 1'].setValues(displayedObject=p)
a = mdb.models['Model-1'].rootAssembly
session.viewports['Viewport: 1'].setValues(displayedObject=a)
session.viewports['Viewport: 1'].assemblyDisplay.setValues(
    optimizationTasks=OFF, geometricRestrictions=OFF, stopConditions=OFF)
a = mdb.models['Model-1'].rootAssembly
a.DatumCsysByDefault(CARTESIAN)
p = mdb.models['Model-1'].parts['Part-1']
a.Instance(name='Part-1-1', part=p, dependent=OFF)
session.viewports['Viewport: 1'].assemblyDisplay.setValues(
    adaptiveMeshConstraints=ON)
mdb.models['Model-1'].FrequencyStep(name='Step-1', previous='Initial',
    numEigen=5)
session.viewports['Viewport: 1'].assemblyDisplay.setValues(step='Step-1')
session.viewports['Viewport: 1'].assemblyDisplay.setValues(interactions=ON,
    constraints=ON, connectors=ON, engineeringFeatures=ON,
    adaptiveMeshConstraints=OFF)
session.viewports['Viewport: 1'].partDisplay.setValues(sectionAssignments=OFF,
    engineeringFeatures=OFF)
session.viewports['Viewport: 1'].partDisplay.geometryOptions.setValues(
```

```
    referenceRepresentation=ON)
p = mdb.models['Model-1'].parts['Part-1']
session.viewports['Viewport: 1'].setValues(displayedObject=p)
p = mdb.models['Model-1'].parts['Part-1']
f, e, d1 = p.faces, p.edges, p.datums
t = p.MakeSketchTransform(sketchPlane=f[4], sketchUpEdge=e[7],
    sketchPlaneSide=SIDE1, sketchOrientation=LEFT, origin=(0.0, 0.0,
    0.003))
s1 = mdb.models['Model-1'].ConstrainedSketch(name='__profile__',
    sheetSize=0.365, gridSpacing=0.009, transform=t)
g, v, d, c = s1.geometry, s1.vertices, s1.dimensions, s1.constraints
s1.sketchOptions.setValues(decimalPlaces=3)
s1.setPrimaryObject(option=SUPERIMPOSE)
p = mdb.models['Model-1'].parts['Part-1']
p.projectReferencesOntoSketch(sketch=s1, filter=COPLANAR_EDGES)
s1.Line(point1=(-0.063, 0.015), point2=(-0.063, 0.00224999995157123))
s1.VerticalConstraint(entity=g[6], addUndoState=False)
s1.PerpendicularConstraint(entity1=g[5], entity2=g[6], addUndoState=False)
s1.CoincidentConstraint(entity1=v[4], entity2=g[5], addUndoState=False)
s1.ObliqueDimension(vertex1=v[4], vertex2=v[5], textPoint=(-0.0449091754853725,
    0.00893950089812279), value=0.015)
s1.DistanceDimension(entity1=g[4], entity2=g[6], textPoint=(
    -0.0643293559551239, 0.0216110274195671), value=0.045)
p = mdb.models['Model-1'].parts['Part-1']
f = p.faces
pickedFaces = f.getSequenceFromMask(mask=('[#10 ]', ), )
e1, d2 = p.edges, p.datums
p.PartitionFaceBySketch(sketchUpEdge=e1[7], faces=pickedFaces,
    sketchOrientation=LEFT, sketch=s1)
s1.unsetPrimaryObject()
del mdb.models['Model-1'].sketches['__profile__']
p = mdb.models['Model-1'].parts['Part-1']
c = p.cells
pickedCells = c.getSequenceFromMask(mask=('[#1 ]', ), )
e = p.edges
pickedEdges =(e[13], )
p.PartitionCellBySweepEdge(sweepPath=e[3], cells=pickedCells,
    edges=pickedEdges)
session.viewports['Viewport: 1'].partDisplay.setValues(sectionAssignments=ON,
    engineeringFeatures=ON)
session.viewports['Viewport: 1'].partDisplay.geometryOptions.setValues(
    referenceRepresentation=OFF)
a = mdb.models['Model-1'].rootAssembly
a.regenerate()
a = mdb.models['Model-1'].rootAssembly
session.viewports['Viewport: 1'].setValues(displayedObject=a)
```

```
session.viewports['Viewport: 1'].assemblyDisplay.setValues(interactions=OFF,
    constraints=OFF, connectors=OFF, engineeringFeatures=OFF)
session.viewports['Viewport: 1'].assemblyDisplay.setValues(
    adaptiveMeshConstraints=ON)
session.viewports['Viewport: 1'].assemblyDisplay.setValues(interactions=ON,
    constraints=ON, connectors=ON, engineeringFeatures=ON,
    adaptiveMeshConstraints=OFF)
a = mdb.models['Model-1'].rootAssembly
f1 = a.instances['Part-1-1'].faces
faces1 = f1.getSequenceFromMask(mask=('[#1 ]', ), )
pickedRegions = a.Set(faces=faces1, name='Set-1')
mdb.models['Model-1'].rootAssembly.engineeringFeatures.assignSeam(
    regions=pickedRegions)
session.viewports['Viewport: 1'].assemblyDisplay.setValues(loads=ON, bcs=ON,
    predefinedFields=ON, interactions=OFF, constraints=OFF,
    engineeringFeatures=OFF)
session.viewports['Viewport: 1'].view.setValues(nearPlane=0.295469,
    farPlane=0.484251, width=0.181722, height=0.0772028, cameraPosition=(
    -0.244355, 0.231552, 0.19815), cameraUpVector=(0.206735, 0.411227,
    -0.88778), cameraTarget=(0.00777249, -0.00413558, -0.00213685))
a = mdb.models['Model-1'].rootAssembly
f1 = a.instances['Part-1-1'].faces
faces1 = f1.getSequenceFromMask(mask=('[#10 ]', ), )
region = a.Set(faces=faces1, name='Set-3')
mdb.models['Model-1'].EncastreBC(name='BC-1', createStepName='Step-1',
    region=region, localCsys=None)
session.viewports['Viewport: 1'].assemblyDisplay.setValues(mesh=ON, loads=OFF,
    bcs=OFF, predefinedFields=OFF, connectors=OFF)
session.viewports['Viewport: 1'].assemblyDisplay.meshOptions.setValues(
    meshTechnique=ON)
a = mdb.models['Model-1'].rootAssembly
e1 = a.instances['Part-1-1'].edges
pickedEdges = e1.getSequenceFromMask(mask=('[#f ]', ), )
a.seedEdgeBySize(edges=pickedEdges, size=0.00045, deviationFactor=0.1,
    constraint=FINER)
a = mdb.models['Model-1'].rootAssembly
e1 = a.instances['Part-1-1'].edges
pickedEdges = e1.getSequenceFromMask(mask=('[#3ead0 ]', ), )
a.seedEdgeBySize(edges=pickedEdges, size=0.0005, deviationFactor=0.1,
    constraint=FINER)
a = mdb.models['Model-1'].rootAssembly
partInstances =(a.instances['Part-1-1'], )
a.generateMesh(regions=partInstances)
session.viewports['Viewport: 1'].view.setValues(session.views['Iso'])
session.viewports['Viewport: 1'].view.setValues(nearPlane=0.331402,
    farPlane=0.466675, width=0.0447377, height=0.0190764,
```

```
    viewOffsetX=-0.0301058, viewOffsetY=0.0253417)
session.viewports['Viewport: 1'].view.fitView()
session.viewports['Viewport: 1'].assemblyDisplay.setValues(mesh=OFF)
session.viewports['Viewport: 1'].assemblyDisplay.meshOptions.setValues(
    meshTechnique=OFF)
mdb.Job(name='UDwithCrack', model='Model-1', description='UD with crack',
    type=ANALYSIS, atTime=None, waitMinutes=0, waitHours=0, queue=None,
    memory=90, memoryUnits=PERCENTAGE, getMemoryFromAnalysis=True,
    explicitPrecision=SINGLE, nodalOutputPrecision=SINGLE, echoPrint=OFF,
    modelPrint=OFF, contactPrint=OFF, historyPrint=OFF, userSubroutine='',
    scratch='', resultsFormat=ODB, multiprocessingMode=DEFAULT, numCpus=1,
    numGPUs=0)
mdb.jobs['UDwithCrack'].submit(consistencyChecking=OFF)
session.mdbData.summary()
```